The University of South Bohemia in České Budějovice

Faculty of Science

Combination of cancer immunotherapy with inhibitors of glutamine metabolism

Bachelor's thesis

Konstantin Kosenko

Supervisor: RNDr. Jan Ženka, CSc.

České Budějovice 2022

Kosenko K. 2022: Combination of cancer immunotherapy with inhibitors of glutamine metabolism. Bc. Thesis, in English, 59 p. Department of Medical Biology, Faculty of Science, University of South Bohemia, České Budějovice, Czech Republic.

Annotation

The focus of this thesis was the combination of immunotherapy with glutamine metabolism inhibitors. Glutamine analogs such as 6-diazo-5-oxo-L-norleucine (DON) have been known for many decades; however, their use has been limited due to severe side effects. In this study, we focused on DON and its prodrug LTP607 and tested its combination with immunotherapy that includes mannan-BAM, Toll-like receptor ligands, and anti-CD40 antibodies in the rather aggressive pancreatic adenocarcinoma model. The main objective of the study was to compare the side effects of DON and its prodrug, to study the efficiency of this combination against secondary tumors, and to evaluate the influence of such a combination on the survival of mice.

Declaration

I declare that I am the author of this qualification thesis and that in writing it, I have used the sources and literature displayed in the list of used sources only.

Linz, 22.07.2022 .....

Konstantin Kosenko

Acknowledgment

First, I would like to express my thanks to my supervisor, RNDr. Jan Ženka, CSc., who supported me from the very beginning, gave me hints, inspiration, and motivation and who was always ready to share his great experience, knowledge, and practical skills with me. In the same way, I am really thankful to Mgr. Radka Lencová for support, all answered questions and help in many aspects throughout the whole project, the help that cannot be overstated. It was always a pleasure to work with you both!

Furthermore, I am grateful to Dr. Pavel Majer from the Institute of Organic Chemistry and Biochemistry of the CAS for his consultation, for his really inspiring meeting, and for his help in providing the molecule LTP607, which was developed by his group and finally tested in this thesis.

In addition, I would like to thank Professor Libor Grubhoffer for his support and motivation throughout the study, for his idea and suggestion to join this wonderful project, and for the biochemistry lectures and the obtained knowledge, which helped many times in this project.

Finally, I want to thank my family, Angi, and friends, who were always there for me and who always gave me support, inspiration, and ideas. These are the most important people in my life who were always ready to listen to me, ready to help, and who believed in me. Without you all, I would never have gone so far!

Table of Contents

1 Introduction

1.1 General background

Today, there are many diseases that people can successfully treat and cure. However, there are still some cases where complete curing is an exception rather than a rule. Cancer therapy often represents exactly this case. Despite the extensive knowledge in the field, successful treatment is still very challenging. One of the reasons behind it is the large variability that cancer presents. Another reason is the number of sophisticated mechanisms cancer uses to avoid and survive any treatment.

Throughout progression, cancer can undergo various genetic and epigenetic changes, allowing it to proliferate and take control of the treatment that is applied. Moreover, cancer cells are generally characterized by a number of hallmarks that allow tumor growth and metastasis. Unlike normal cells and tissues, cancer cells, for example, are known to sustain proliferative signals which allow them to proliferate uncontrollably [36]. Furthermore, many genes that negatively regulate cell proliferation are inactive in cancer cells. Thus, cancer cells are known to evade growth suppressors [36].

In addition, cancer cells can deregulate cell death by resisting apoptosis. The hallmark is quite significant because it can give cancer cells resistance to many therapeutic agents that kill cells by inducing apoptosis in them [2]. Besides that, unlike normal cells, cancer cells were shown to upregulate telomerase which prevents telomere shortening [15]. This ability allows cancer cells to avoid senescence and go through an unlimited number of cell division cycles. [15, 36].

Another significant difference between cancer and normal cells is the ability of cancer cells to form metastases and invade other tissues. This hallmark is particularly important because metastasis is the primary cause of cancer-related deaths [25]. Furthermore, each organism is different and unique and thus gives a different response to the same treatment. Therefore, this complex disease remains a topic of interest for many researchers. In this thesis, I would like to give an overview of the basic knowledge of the topic that is known and that is not.

1.2 Immune system in cancer immunotherapy

There are several ways in cancer therapy: surgery, radiation therapy, chemotherapy, immunotherapy, and a combination of previously stated approaches. Discovered in 1891 by Dr. William Coley, immunotherapy remains the least studied and most promising approach to

treating cancer [1, 77]. The approach (immunotherapy) is based on the stimulation and targeting of the immune system, which in turn results in the elimination of pathogenic cells, including cancer cells [59]. Depending on the mechanism of action and the types of cells included, the immune system can be divided into innate immunity and adaptive immunity [6].

1.3 Innate immunity: fast and general defense

The innate immune response involves a set of different mechanisms that begin to act immediately (within minutes or hours) after the pathogen is invaded [51]. Unlike adaptive immunity, innate immunity provides a general defense (nonspecific) and includes almost any cell type [6]. It can be divided into four main barriers: physical barriers (e.g., epithelial surface, mucus layer), physiological (temperature, low pH in the stomach), endocytic and phagocytic, and inflammatory [26, 51].

Cells involved in the innate immune response can recognize pathogenic cells using pattern recognition receptors (PRRs) that detect repeating patterns that are called pathogen-associated molecular patterns (PAMPs) [6, 51]. Furthermore, PRRs also detect the presence of molecules called damage-associated molecular patterns (DAMPs), which have an endogenous origin and result from damaged cells [71].

Today, four different types of PRRs have been recognized, including Toll-like receptors (TLRs) and C-type lectin receptors (CLRs), which are transmembrane proteins and cytoplasmic proteins such as Retinoic acid-inducible gene (RIG)-I-like receptors (RLRs) and NOD-like receptors (NLRs) [71]. Transmembrane PRRs can be located within the plasma membrane or the endolysosomal system. These PRRs can be found in various types of cells, including non-professional immune cells.

1.4 The role of TLRs in immune response

All PRRs recognize distinct ligands. For example, mammals express at least ten different TLRs that recognize molecular patterns such as lipoproteins, double-stranded RNA (dsRNA), single-stranded RNA (ssRNA) (Figure 1), and other ligands [71]. Some TLRs can recognize more than one ligand, and some of them can form heterocomplexes with other TLRs [14]. That considerably expands the repertoire of molecular patterns that can be detected. Activation of these receptors results in the production of extracellular signal molecules that induce an inflammatory response [6]. Inflammation can be defined as a response of the organism to noxious and potentially dangerous conditions that include tissue injury and infection [56]. It can often be characterized as redness, swelling, heat, or pain. Blood vessels become permeable, allowing immune cells, such as neutrophils, to escape to inflamed areas where they

fight pathogens [55]. The signal molecules, which are produced upon activation of PRRs, include proinflammatory cytokines, type I interferons (IFNs), chemokines, vasoactive amines, eicosanoids (e.g., prostaglandins), and others [56, 71]. Different PRRs result in different patterns of signal molecules [71].

1.5 Signaling pathways of TLRs

As mentioned earlier, the activation of PRRs results in the expression of many genes, including proinflammatory cytokines. There are two main domains in all TLRs: **the extracellular domain**, which consists of leucine-rich repeat (LRR) motifs and which is responsible for the recognition of corresponding ligands, and **the intracellular domain,** which is called Toll/IL-1R (TIR) domain since this domain is structurally similar to intracellular domains of interleukin-1 receptors (IL-1Rs) [5].

Once the ligand has been bound to the LRR domain, the receptors dimerize, and the conformation change allows the recruitment of signaling molecules. The following signaling molecules have been determined: myeloid differentiation primary response protein 88 (MyD88), transforming growth factor-β (TGF-β)-activated kinase (TAK1), TAK1-binding protein 1 (TAB1), TAB2, IL-1R-associated kinases (IRAKs), and tumor-necrosis factor (TNF)-receptor-associated factor 6 (TRAF6) [31]. The activation of TLRs by ligands results in a consequent transfer of signal that ultimately leads to the release of nuclear factor κB (NF- κB) [46]. Nuclear translocation of NF- κB leads to the subsequent transcription of many target genes, including genes that encode inflammatory cytokines, antimicrobial peptides, chemokines, and others [45, 79].

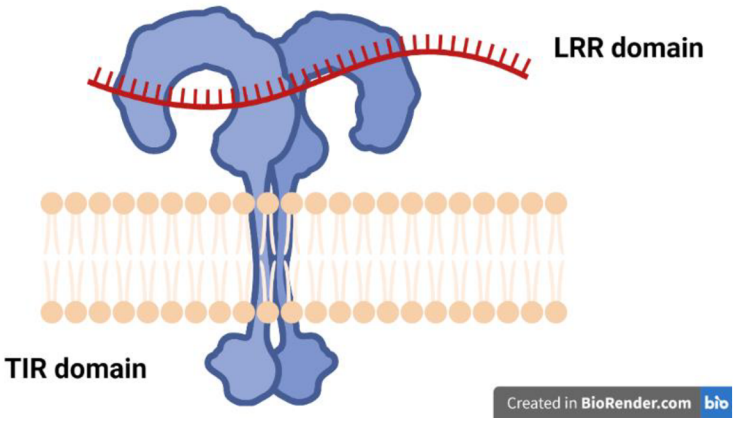

Figure 1: Toll-like receptor with bound ssRNA (shown in red)

1.6 Cells of innate immunity

1.6.1 Macrophages

Innate immunity relies on many cell types, and some of these cells serve various functions (not only the immune function). For example, intestinal epithelial cells provide absorption of nutrients, barrier function, and, finally, immune function (cytokine secretion) [67]. However, there are some cells that are considered professional immunocytes. These cells are part of myeloid cells and include mononuclear phagocytes (macrophages and dendritic cells) and polymorphonuclear leukocytes (PML) (neutrophils, basophils, and eosinophils) [14].

Macrophages are long-lived phagocytes, and they are among the first cells that detect pathogens by means of PRRs that recognize PAMPs and DAMPs. Once the pathogen has been encountered, macrophages engulf and kill it. Furthermore, macrophage-released cytokines recruit other myeloid cells, such as polymorphonuclear leukocytes [14]. Once the pathogen has been engulfed, phagocytic cells (macrophages and neutrophiles) generate different toxic reactive species to kill the engulfed pathogens (Figure 2). The generation of reactive species such as hypochlorous acid (HOCl), hydroxyl radical ($OH^{\bullet}$), peroxynitrite ($ONOO^{-}$), and singlet oxygen ($^{1}O_2$) is initiated by the NADPH oxidase complex [14]. The reactions which are described in Figure 2 and are required for the generation of reactive oxygen species (ROS) demand a high consumption of oxygen. This phenomenon is called a respiratory burst [29].

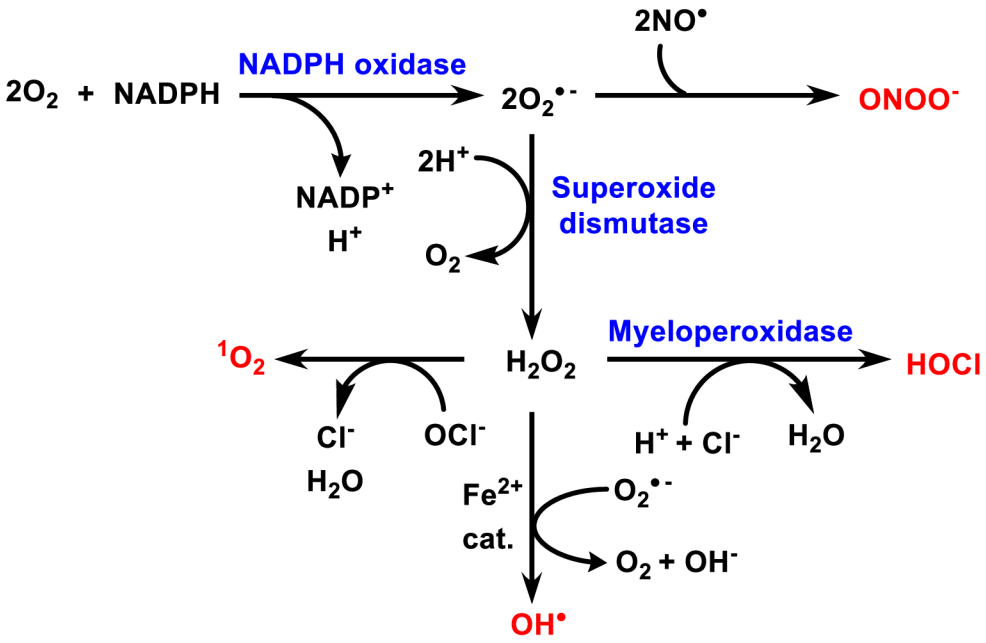

Figure 2: Reactive species generated by phagocytes to kill pathogens [14]

1.6.2 Neutrophils

Particular attention should be paid to the previously mentioned neutrophils. These cells are the most abundant cell types in the blood, and their role is not limited to just the killing of pathogens [66]. They also produce cytokines, regulate macrophages for long-term responses, regulate inflammation itself, and play an important role in many diseases, including cancer [66]. Therefore, speaking of cancer immunotherapy, it is essential to discuss the role of neutrophils in cancer development. Despite being the most abundant type of leukocyte (neutrophils represent around 70% of all leukocytes), only 1-2% of all neutrophils circulate in the blood [66].

Neutrophils can escape from the blood to the site of inflammation through a process which is called the leukocyte adhesion cascade [66]. The process includes four main steps: selectin-dependent tethering and rolling of leukocytes, activation of leukocytes with chemokines, firm adhesion mediated by integrins, and finally, transcellular migration of leukocytes [27]. Once neutrophils escape from blood vessels, they follow a gradient of molecules such as formyl-methionyl-leucyl-phenylalanine (fMLF) and anaphylatoxin C5a (which will be discussed later) [66].

Inflammation plays a critical role in the process of the leukocyte adhesion cascade. Selectins are glycoproteins that mediate interactions between leukocytes or platelets with the endothelial vascular surface [54]. There are three types of selectins which are called L-, P-, and E-selectins. L-selectin can be found on the surface of most leukocytes. E-selectin is expressed upon activation by cytokines on endothelial cells. The last P selectin is found on the surfaces of endothelial cells and platelets [54]. The rolling and tethering of leukocytes are mostly mediated by the interaction of E- and P-selectins of endothelial cells with P-selectin glycoprotein-1 (PSGL-1), which is expressed on leukocytes. Both P- and E-selectins are exposed to the surface only upon inflammatory stimuli. Furthermore, chemokine-induced activation is necessarily for the integrin-mediated firm adhesion, which is the crucial stage of the whole process [27].

1.6.3 Neutrophils and cancer

The role of neutrophils in the immune response cannot be overstated. However, it should be mentioned that their contribution is not always positive. For example, ROS, which they use to eliminate pathogens, are not specific and responsible for tissue damage [84]. Furthermore, due to the plasticity and diversity that neutrophils demonstrate, they can even perform an immunosuppressive function inhibiting T-cell immunity [84]. Cancer is not an exception here, and, as was shown in many experiments, some neutrophils possess antitumor activity (so-

called N1 subpopulation), and some neutrophils demonstrate protumor function (so-called N2 neutrophils) [70]. In addition, recent discoveries suggest that tumor microenvironments appear to be capable of reprogramming neutrophils (through the action of different signal pathways, cytokines, and other factors), transforming them into tumor-promoting cells [84]. Moreover, the increased number of neutrophils in the blood during cancer progression is often associated with poor prognosis [66].

1.6.4 Dendritic cells provide the link between innate and adaptive immunity

Another type of cell that should be mentioned in the context of innate immunity is dendritic cells (DCs). Among the different subpopulations of dendritic cells, special attention should be paid to conventional type 1 dendritic cells (cDC1) because their action on cancer cells is well-studied and rather significant. In different experiments, depletion of cDC1 has been shown to lead to the inability to reject transplantable tumors and to the absence of efficiency of T cell-based immunotherapy [19]. Furthermore, even though these cells are generally not abundant in tumors, their elevated number in the tumor microenvironment (TME) often predicts a good prognosis in some cancers [20].

cDC1s can be attracted into TME by various chemokines (such as CCL4, CCL5, and XCL1) expressed by the tumor itself or by NK cells. In this way, NK cells play an important role in recruiting cDC1s. In addition, NK cells produce growth factors such as the fms-like tyrosine kinase 3 ligand (FLT3L) that also attract cDC1 to TME [18].

It has been shown that cDC1s have a specific role in cancer suppression. Firstly, cDC1s present tumor peptides to naïve T cells, generating this way cytotoxic effector $CD8^+$ T cells [19]. T cell priming (even though it can be done in TME) mainly occurs primarily in tumor-draining lymph nodes through migratory cDC1s [19]. These cells possess a unique ability to deliver antigens with minimal degradation of this antigen and the ability to expose the antigens to be presented [19]. Within TME, cDC1s serve yet another function. They produce different chemokines, such as CXCL9 and CXCL10, recruiting T cells and NK cells into TME [19]. Furthermore, they produce the cytokine IL-12, which stimulates the cytotoxic activity of $CD8^+$ T cells [19].

As could be expected, there are several mechanisms utilized by tumors to diminish the activity of cDC1s. For example, TGF-β, produced by various tumors, reduces the ability of cDC1 to produce cytokines and to take up antigens, significantly lowering their function [39].

1.7 Complement system

1.7.1 The role of the complement system in immune response

The complement system is an essential part of the innate immune system, which plays an important role in the elimination of foreign cells (pathogens) and the elimination of apoptotic cells. It can be represented as a cascade of reactions that results in the opsonization of pathogenic cells, the recruitment of immune cells, and the mediation of inflammation or direct killing by means of apoptosis [58].

It is worth mentioning that complement is considered an important mediator between innate and adaptive immunity. Opsonization marks pathogens for antigen-presenting cells (APCs), which engulf them and modulate B- and T-cell responses [58]. The complement system is composed of more than forty proteins, including soluble proteins (made by the liver) and membrane-bound proteins [58]. Usually, it is divided according to the activation mechanism into three pathways: classical, alternative, and lectin. The core component of all pathways is C3. It can be cleaved into the C3a and C3b fragments. C3b acts as an opsonization tool, and its presence on the pathogen surface promotes phagocytosis of the cell and stimulates B cells of adaptive immunity. C3a is a smaller fragment and plays an essential role in the recruitment of other immune cells to the inflammation site [6].

1.7.2 Activation of complement pathways

Alternative pathway is a pathway that predominates under normal physiological conditions where it can be spontaneously activated by hydrolysis of a thioester bond that converts C3 to C3(H_2O). Hydrolysis induces conformational changes, which in turn allow for the recruitment of Factor B (FB). Once FB has been bound, the whole complex is a substrate for a serine protease called factor D (FD), which yields the convertase complex C3bBb [45]. The complex cleaves C3 into C3a and C3b. As mentioned above, the C3b component participates in opsonization and can bind covalently to the hydroxyl group via its thioester domain (TED) [57]. Healthy host cells possess a set of regulators that inactivate C3b, preventing apoptosis. On the other hand, apoptotic cells have decreased expression of complement regulators on the cell surface. Speaking of pathogens, they often lack those complement regulators at all [57] and thus are more vulnerable to the action of the complement system.

Classical pathway is activated by the C1q protein complex [34]. The complex is produced by monocytes, immature dendritic cells, and macrophages and provides a vast number of immune functions. The multifunctionality of the component can be explained by many ligands that can interact with the C1q complex, mostly via ionic interactions. For

example, as it was already mentioned, the complex activates the classical pathway of complement, which is triggered by antigen-bound immunoglobulin G (IgG) or immunoglobulin M (IgM). In addition, it participates in bacterial clearance, virus inactivation, induction of pro-inflammatory cytokines, chemotaxis (recruitment of neutrophils), and other immune functions [38].

Lectin pathway activation is mediated by Mannose-Binding Lectin (MBL), a protein that recognizes carbohydrates. It has been discovered that MBL has a general structure similar to C1q [33] (Figure 3). Both C1q and MBL associate with complexes of serin protease (SP) called C1r, C1s [49], and MBL-associated serine proteases (MASP) [73]. The association is mediated by Ca^{2+} ions. After that, SPs cleave the complement components C4 and C2, resulting in the C4b2a complex, which is the C3 convertase for classical and lectin pathways [57].

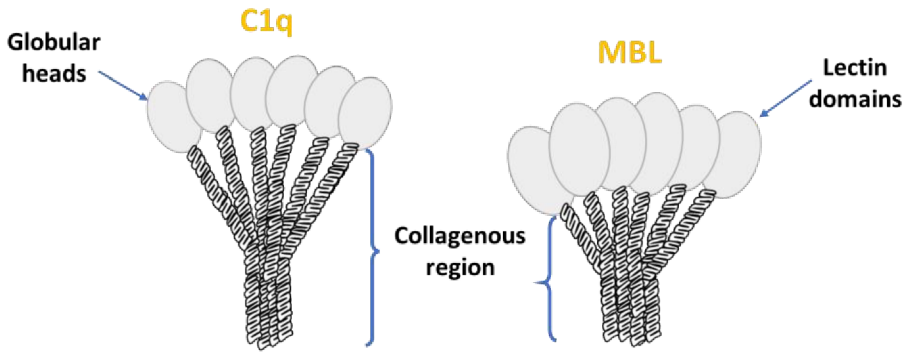

Figure 3: Schematic representation of C1q and MBL [16, 33]

The cleavage of component C3 results in C3a and C3b. C3b can bind to C3 convertase, forming C5 convertase, which cleaves C5, producing C5a and C5b. Then C5b recruits complement components C6, C7, C8, and C9 that polymerize to form the membrane attack complex (MAC) [21]. MAC is a cytotoxic pore that disrupts lipid bilayers. Cell death can result from osmotic flux across the membrane [13]. Sometimes, a single insertion of a functional MAC is sufficient to lyse the cell. This is the case with metabolically inert cells (e.g., erythrocytes) or some gram-negative bacteria. On the other hand, in the case of metabolically active cells, multiple MACs must be inserted to cause lysis [57].

Small fragments C3a and C5a previously mentioned are called anaphylatoxins. These molecules support inflammation (for example, by modulating cytokine expression), recruit immune cells, and induce an oxidative burst in macrophages, eosinophils, and neutrophils [57]. Furthermore, C5a increases phagocytosis, mediates the release of granule enzymes, and acts as a vasodilator [35].

1.7.3 Regulation of the complement system

As expected, the complement system must be tightly regulated to prevent the attack and elimination of health host cells. In addition to positive regulation (using a set of different activators), there is also negative regulation, represented by various inhibitors. These inhibitors (also called complement regulatory proteins (CRPs)) are generally divided into soluble and membrane-bound regulators [63]. For example, soluble serine protease factor I (FI) cleaves C3b and C4b in the presence of certain cofactors [57]. Another soluble regulator is factor H (FH). It competes with FB for binding to C3b and acts as an inhibitor of C3 convertase in the alternative pathway [57]. Furthermore, the MAC formation can be regulated. For example, through CD59, that blocks the formation of pores within the membrane [57]. MAC can also be removed by yet another mechanism, including exocytosis or internalization followed by degradation [57].

1.7.4 The role of complement in tumor progression

Surprisingly, despite being a crucial part of the immune system, the role of the complement system in cancer progression is not unambiguous and straightforward. It is most likely that the complement can acquire both antitumor and protumor character.

According to the review by Rio et al., there is no direct evidence that the complement system can eliminate tumors [63]. The assumption that complement could be helpful against tumor formation is based on the idea that cancer cells must undergo certain genetic and epigenetic alterations to acquire the malignant character [63]. These alterations unavoidably lead to the appearance of certain exposed molecules that allow us to distinguish cancer cells from healthy cells [63]. Nevertheless, there is some indirect evidence that implies that the complement system participates in tumor elimination. The positive effect of the complement system has been appreciated in therapies utilizing monoclonal antibodies (mAb) [11]. Furthermore, complement activation was shown to be an essential condition for the therapeutic activity of some mAbs [30]. Complement-dependent cytotoxicity (CDC) in the case of mAb therapy is based on the following mechanisms: activation of classical pathway and formation of the MAC complex; antibody-dependent cell-mediated cytotoxicity (ADCC), involving the participation of natural killer cells (NK) and neutrophils; and antibody-dependent phagocytosis [64, 72].

Furthermore, as mentioned previously, complement activation leads to the formation of anaphylatoxins that attract phagocytes and improve phagocytosis and ADCC [72]. Another fact that leads to the conclusion that complement might eliminate tumors is the overexpression

of membrane-bound CRPs by cancer cells, which inhibit complement activity [11]. Moreover, CD59 overexpression is associated with a poor treatment prognosis [11].

On the other hand, there is plenty of evidence to suggest that complement activation promotes tumor growth rather than inhibits it. For example, C5a has been shown to modulate tumor growth by attracting myeloid-derived suppressor cells (MDSCs) and reducing the number of cytotoxic T cells [3]. Activation of the C3a receptor (C3aR) supports metastatic behavior, playing a certain role in processes such as cell migration and epithelial-mesenchymal transition [3]. Another experiment has shown that depletion of C3 enhances the ability of certain mAbs to activate NK cells and improve mAb therapy [80]. Finally, the accumulation of MAC (in a certain concentration) promotes cell proliferation and differentiation and inhibits apoptosis [3].

Figure 4 shows the scheme of the complement cascade. To sum it up, there are many contradictions in existing data dedicated to the role of complement in cancer progression. The overall effect is most likely to depend on multiple factors, such as the type of cancer, subpopulations of cells involved in the process, the type of therapy, and many other conditions.

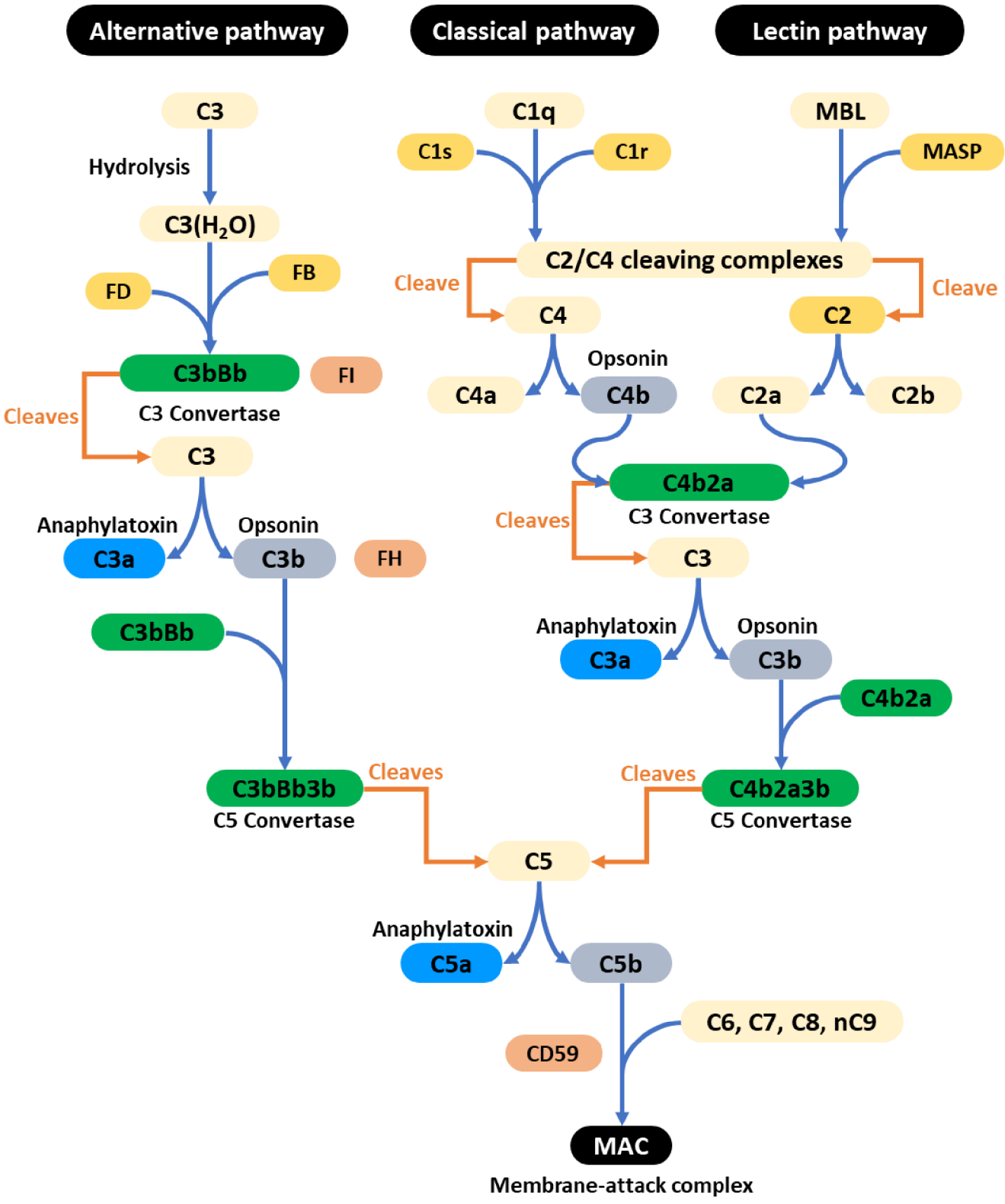

Figure 4: Complement system [49, 64]

1.8 Adaptive immunity

1.8.1 Overview

As was already mentioned, there is a second type of immunity called adaptive immunity. The adaptive immune response starts to act later than the innate immune response but is more

sophisticated, specific, and efficient [6]. Adaptive immunity depends on T and B lymphocytes: T cells mature in the thymus, and B cells develop in the bone marrow [17]. Both cells originate from hematopoietic stem cells that develop into a common lymphoid progenitor cell [6].

B cells produce antibodies and are responsible for the antibody response [6]. T cells serve another function; they detect pathogens and kill them or regulate the activity of other immune cells (such as dendritic cells, macrophages, B cells, and cytotoxic T cells), activating or suppressing them [6].

Because in cancer research, most studies focus on the T-cell-mediated response, T cells will be the primary topic of discussion in this thesis [28]. Upon activation by antigens in peripheral lymphoid organs (such as lymph nodes), T and B cells become morphologically distinguishable from each other: B cells develop an extensive rough endoplasmic reticulum to make antibodies [6]. Furthermore, the activation of the lymphocyte by antigen induces the proliferation of this lymphocyte. The process is called clonal expansion and results in many copies of lymphocytes that recognize the same antigen [6].

1.8.2 Variability of T-cell and B-cell receptors

As mentioned above, adaptive immunity is much more specific than innate immunity. The number of PAMPs recognized by PRRs is relatively limited, whereas B and T cells can specifically recognize almost any antigen. The variability is determined by a sophisticated mechanism, which results in T-cell receptors (TCRs) and B-cell receptors (BCRs). For example, TCRs are Ig-like heterodimers consisting of either α and β chains or γ and δ chains [17]. Each chain consists of two domains: a constant domain and a variable domain. Each β and δ chain is encoded and assembled from three gene segments that are called V (variable), D (diversity), and J (joining) gene segments [17]. The same is true for the α and γ chains, with the only difference being that they are encoded by only the V and J gene segments [17]. These segments are spliced together by means of V(D)J recombinase [17]. From many different segments of the V gene and many segments of the J gene, only one segment of the V gene and one of the J gene are randomly joined to form α (or γ) chain [17]. That contributes to combinatorial diversification. The second mechanism that increases the repertoire of produced TCRs is called junctional diversification. It arises from mutations when DNA segments are joined to each other [17].

1.8.3 Activation and development of T cells

In contrast to B cells, T lymphocytes require activation by dendritic cells that process and present antigens to them [9]. DCs use major histocompatibility complex (MHC) to bind

foreign peptides and present them to TCRs on T lymphocytes. In addition, mature DCs express molecules that promote co-stimulatory and adhesive effects to activate T lymphocytes [9]. Furthermore, DCs produce a variety of cytokines that regulate the activity of many T cells [9].

There are three main classes of T lymphocytes. These are called cytotoxic T cells, helper T cells, and regulatory T cells [6]. Here at this point, it makes sense to clarify the difference between them and their development. In the thymus, bone marrow progenitors undergo TCR rearrangement, which results in double-positive thymocytes (cells that express CD8 and CD4 co-receptors) [41]. There they interact with cells expressing self-peptides bound to MHC complexes. Thymocyte survives only if its TCR binds to the self-peptide-MHC complex with appropriate affinity [6]. The process is called positive selection. Eventually, depending on the preferences for class I or class II MHC proteins, DNA methylation silences the co-receptor (either CD8 or CD4) that is not needed [6]. Thus, single positive thymocytes are formed [6]. Eventually, $CD8^+$ cells develop into cytotoxic T cells (T_C) that bind to class I MHC, while $CD4^+$ cells develop into helper (T_H) and regulatory T cells (T_{reg}) that recognize class II MHC [6].

1.8.4 Co-stimulatory proteins in adaptive immunity

When naïve T cells recognize their antigens (on the surface of dendritic cells), they proliferate and differentiate into effector cells and memory cells [6]. However, the signaling mediated by TCRs that recognize the MHC complex is insufficient for this process. In addition, co-stimulatory proteins are required. The same holds for B cells: effector T_H cells use a CD40 ligand that binds to the CD40 receptor located on the B cell [6]. In addition, this CD40 ligand has two other functions: it acts on dendritic cells, sustaining their activation, and it also helps to stimulate infected macrophages to destroy the pathogen they have [6]. CD40 activation has also been shown to assist immune activation independently of innate immune receptors such as TLRs [79]. Not surprisingly, CD40 agonists such as anti-CD40 mAbs have found their application in cancer therapy [32].

1.9 MBTA immunotherapy

There are many developed immunotherapies that are intensively applied to treat cancer. Many of them represent a mixture of certain compounds which act together to provoke the immune response. Mannan-BAM, TLR ligands, and anti-CD40 mAbs (MBTA) immunotherapy is not exception here [48]. Each component in this mixture plays its own important role.

Mannan (Figure 5) is a polysaccharide that can be obtained from the cell walls of some yeasts [47]. The main chain consists of α-(1→6) linked mannose residues to which side chains

are adjacent via α-(1→3) and α-(1→2) linkages [47]. However, the exact degree of branching and length of the chains are currently unknown [47]. What is known is that mannan connected to **the biocompatible anchor for cell membrane (BAM)** (the approach will be discussed later) can stimulate the phagocytosis and lectin pathway of the complement system [48] via MBL stimulation, as previously discussed.

The TLR ligands in MBTA therapy include the following compounds: **resiquimod (R-848)**, **polyinosinic-polycytidylic acid (poly(I:C)),** and **lipoteichoic acid (LTA)** [48]. **R-848** is an agonist for TLR7/8, which are located in the endolysosomal system and naturally recognize ssRNA [71]. **Poly(I:C)** is a TLR3 agonist and mimics viral dsRNA [71]. The combination of these two TLR ligands has been appreciated in several studies [8, 22]. Furthermore, it has been shown that this combination showed better efficacy in the activation of antitumor macrophages and cytokine production compared to individual application of each TLR agonist separately [8]. The last TLR ligand is **LTA**, which stimulates TLR2 and mimics some viral and bacterial lipoproteins [71, 77]. The last component of the MBTA mixture is anti-CD40 mAbs, already discussed above [48].

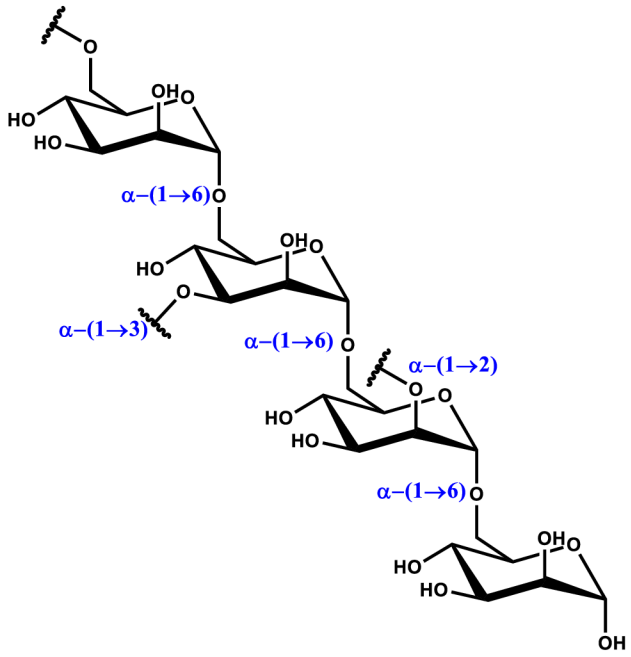

Figure 5: principal structure of mannan. The main chain consists of mannose residues linked through α-(1→6) linkage. Branching from the main chain is performed through α-(1→3) and α-(1→2) linkages [47].

1.10 Combination of MBTA immunotherapy with other therapies

In nature, cancer often tends to produce metastases and secondary tumors. These tumors are usually less reachable than the primary ones. A two-tumor model can be used to simulate such

a situation. In this case, one tumor is treated with therapy and considered the primary one, while the second tumor is nontreated and represents the secondary formation.

Although MBTA immunotherapy showed its efficiency in one tumor model, immunotherapy alone was insufficient to eliminate non-treated tumors in two tumor models [78]. Therefore, the combination of MBTA therapy with another type of treatment should be considered, and this has eventually become the aim of this thesis. In this study, we focus on the combination with glutamine metabolism inhibitors such as 6-Diazo-5-oxo-L-norleucine (DON). The reasons behind this choice will be explained in the following. First, the features of glutamine metabolism in cancer cells should be considered.

1.11 Glutamine metabolism and role in cancer cells

Although it is only a conditionally essential amino acid, glutamine plays an important role in the metabolism of many cells and especially rapidly proliferating cells such as lymphocytes, enterocytes, and cancer cells, where it serves as a source of carbon, nitrogen, and energy to meet anabolic demands [7]. In fact, increased uptake of glutamine in cancer cells was observed in several studies. For example, up-regulation and overexpression of some glutamine transporters (such as SLC1A5) [68] and glutamine using enzymes (such as glutaminase) [53] were confirmed and can be considered as proof of the importance of glutamine for cancer cells.

As mentioned earlier, glutamine is an important amino acid for rapidly proliferating cells. First, it is a source of metabolic energy (Figure 7). Within the cell, glutamine can be converted to glutamate by glutaminases (GLS/GLS2). In turn, glutamate can be converted to alpha-ketoglutarate (α-KG), which can enter the citric acid cycle (also known as the Krebs cycle) in order to generate ATP and NADH, and $FADH_2$ molecules that can be used in oxidative phosphorylation [7]. The conversion to α-KG is catalyzed by glutamate dehydrogenase (GLUD) or aminotransferases.

Furthermore, the previously mentioned α-KG can be used in reductive carboxylation, the reaction catalyzed by isocitrate dehydrogenase (IDH) that generates citrate (Figure 8), which can be used in lipid metabolism in cancer cells under certain conditions, such as hypoxia [7, 83]. Moreover, glutamine-deficient hypoxic cells cannot proliferate efficiently [83]. In addition, glutamine contributes to the production of glutathione (GSH), the most abundant antioxidant in the organism [10]. Cancer cells utilize glutathione to remove ROS, which can otherwise damage biomolecules and eventually lead to cell death [10]. In several studies, elevated levels of GSH have been shown to be associated with metastasis in various types of

cancer [10]. Glutathione is a tripeptide that requires glutamate, cysteine, and glycine [10]. As mentioned above, glutamine can be converted to glutamate, which is used directly in GSH synthesis (Figure 9), and furthermore, its outflow is required for cystine influx via the xCT transporter [10]. Cystine can then be converted to cysteine [40]. Moreover, the xCT transporter is up-regulated in many cancers and promotes tumor growth [40]. Finally, glutamine is essential for nucleotide biosynthesis (and, therefore, proliferation), and its deprivation is associated with an increased level of cell death [81]. Figure 6 shows which nitrogen atoms in nucleotides are derived from glutamine [42]. All given examples indicate and support the importance of glutamine for fast-proliferating cells, such as cancer cells, and its role can hardly be overstated.

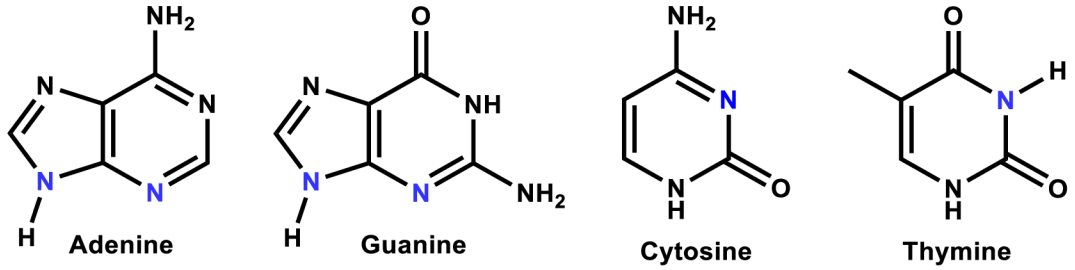

Figure 6: The nitrogen atoms shown in blue are derived from glutamine [42]

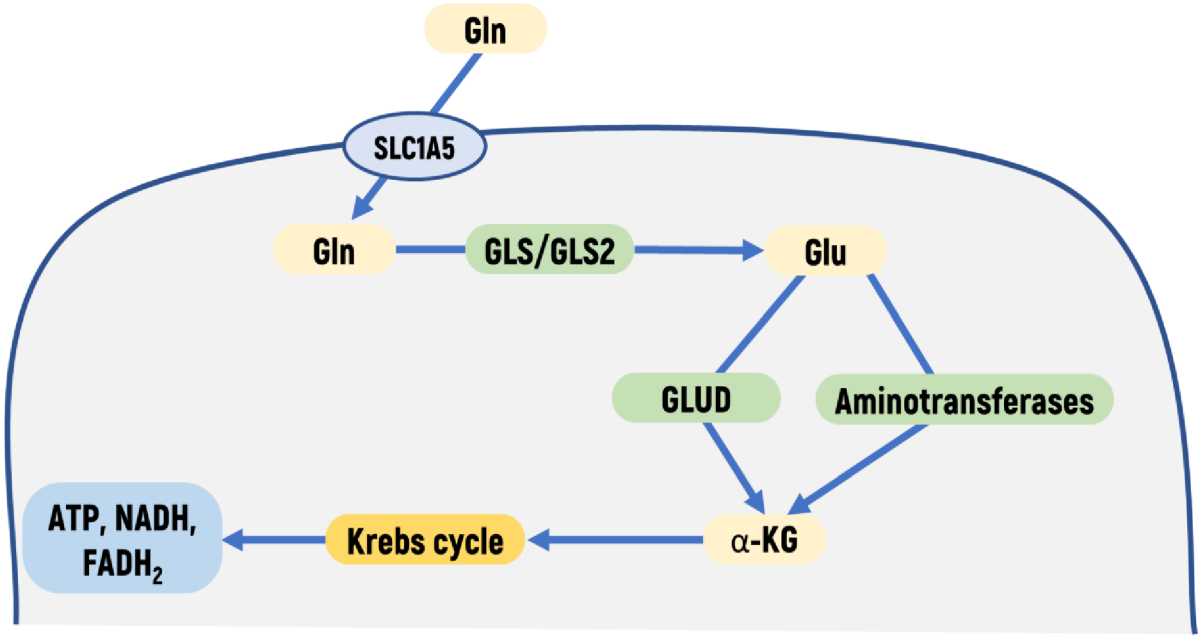

Figure 7: Glutamine as an energy-generating substrate [7]

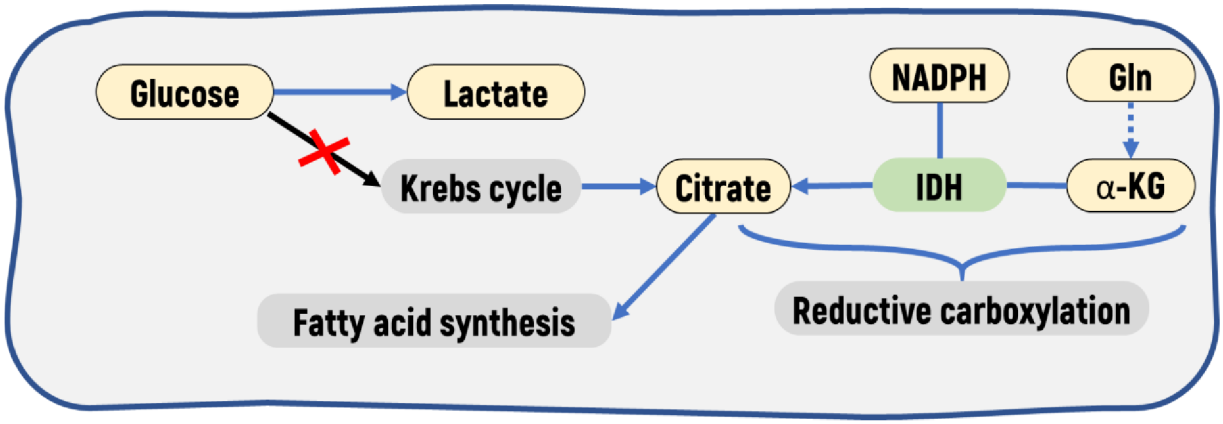

Figure 8: Glutamine as a substrate in fatty acid synthesis (α-KG is obtained the same way as was shown in Figure 7)

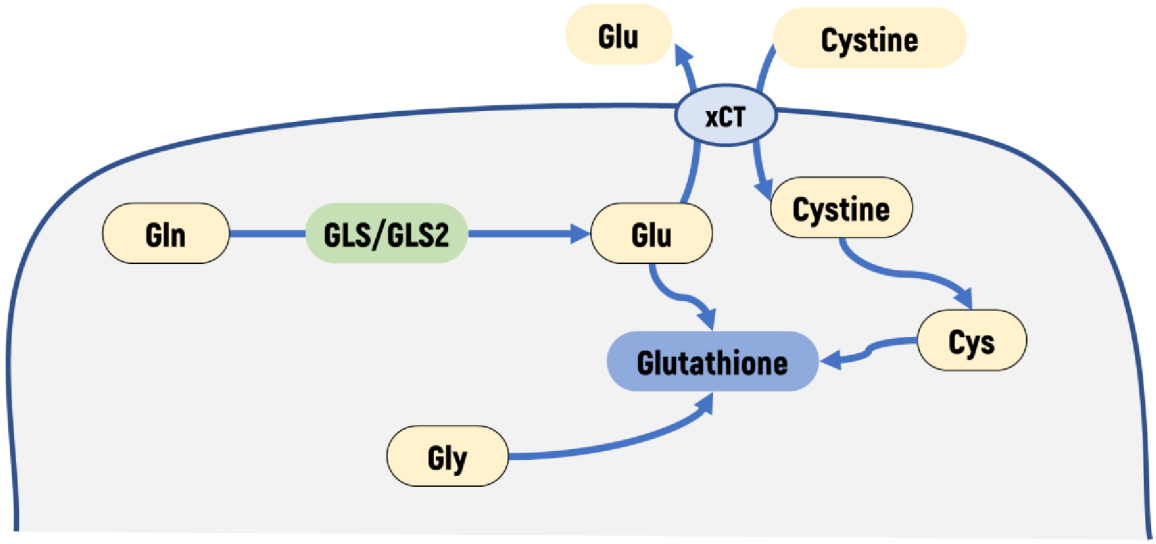

Figure 9: Glutamine contributes to glutathione biosynthesis

1.12 Glutamine metabolism as a target in cancer therapy

As expected, because of its significance in fast-dividing cells, glutamine metabolism has become a target in certain cancer therapies. There are different ways to inhibit glutamine metabolism. Some ways include the inhibition of glutamine using enzymes such as GLS, GLUD, or glutamine-conducting transporters such as SLC1A5 or xCT [7]. Furthermore, there is a group of compounds that are considered glutamine analogs and include the previously mentioned DON, azaserine, and acivicin [7]. These three compounds efficiently inhibit the steps in nucleotide biosynthesis that involve enzymes that use glutamine [82]. However, despite the significant antitumor cytotoxic activity, the use of these compounds has been stopped due to side effects that include gastrointestinal (GI) toxicity and neurotoxicity [82]. Nevertheless, there are some possibilities that allow us to overcome the undesirable side

effects. One way is to use prodrugs, compounds that are generally not active until they do not get into the target cells, where the active form is liberated [76].

1.13 DON broadly inhibits glutamine metabolism

In this study, we focus on DON and its prodrug to test the synergetic effect and its compatibility with MBTA therapy. Thus, it is worth mentioning to elaborate on the mechanism of action of DON inside the cell and what is hidden behind its cytotoxic efficiency. As mentioned above, DON is a glutamine analog (as well as azaserine, Figure 10), and once inside the cell, it competitively binds the active site to a wide range of glutamine-utilizing enzymes such as glutaminase, glutamine amidotransferases involved in nucleotide biosynthesis, and others [43]. Subsequently, DON forms a covalent bond with the enzyme, irreversibly inhibiting it this way [43].

It is worth mentioning that DON is stable under cellular conditions until its diazo group is protonated [43]. The protonation makes it highly electrophilic (partly because of the presence of a good leaving group, N_2) [43]. Thangavelu et al. revealed that such a protonation could be done by a serine residue in the proximity of the active center in kidney-type glutaminase (KGA), for example [75]. The mechanism of this activation is shown in Figure ***11***.

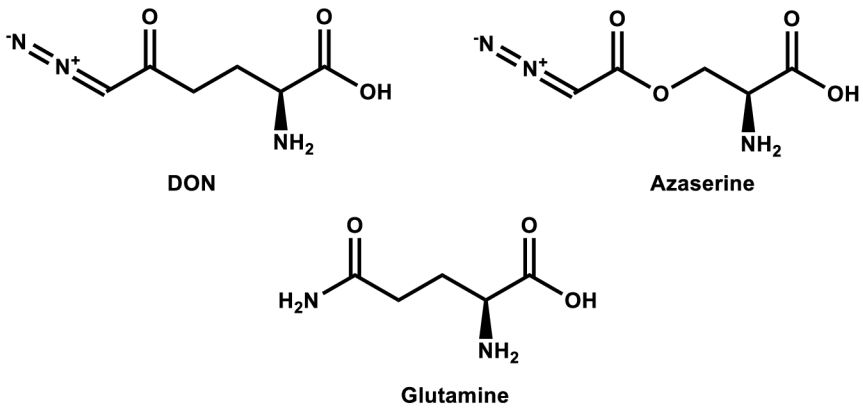

Figure 10: DON and azaserine are structural analogs of Gln

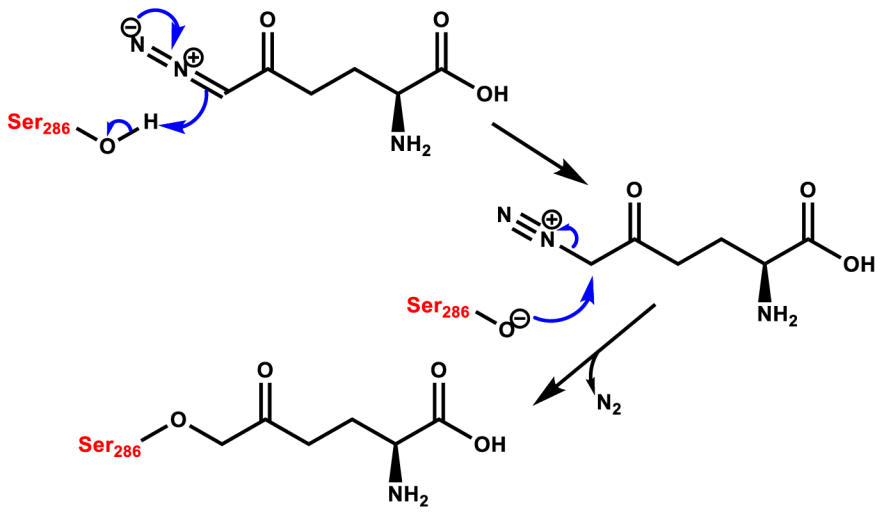

Figure 11: Mechanism of inhibition of KGA (serine residue 286) by DON

1.14 Side effects limit the application of DON: solution

However, as already mentioned, despite the apparent antitumor effect, the application of DON is limited, mainly due to GI toxicity. Symptoms such as nausea, vomiting, diarrhea, and GI bleeding were often observed in clinical trials and were the main restricting factors in the application of DON [43]. Rapidly proliferating epithelial GI cells are also dependent on glutamine and, as a consequence, are susceptible to DON, as observed in clinical trials [43].

Thus, many prodrugs of DON have been developed to obtain higher specificity and fewer side effects. One approach is to utilize tumor-specific enzymes that release the prodrug releasing the active form only inside the tumor. Ueki et al. showed that two of such specific enzymes are histone deacetylase (HDAC) and protease cathepsin L (CTSL) [76]. It should be mentioned that these enzymes are not unique solely to the tumor but play a special role in tumor progression and metastasis and, thus, are quite often up-regulated and overexpressed [76]. The idea was to connect the drug with the N-acetyl lysine residue [76]. First, the acetyl group is supposed to be removed by HDAC, and then the Lys residue is cleaved by CTSL, releasing the active form of the drug [76].

A similar approach has been applied to develop DON derivatives in the Institute of Organic Chemistry and Biochemistry, Academy of Sciences of the Czech Republic [74]. The best prodrug 6 (in the future will be referred to as LTP607, Figure 12) showed rapid release of DON in tumors. At the same time, the stability of the prodrug in the intestine provides reduced side effects typical of DON itself [74]. Thus, the hypothesis that LTP607, due to its reduced toxicity, can be successfully combined with MBTA therapy has been formulated.

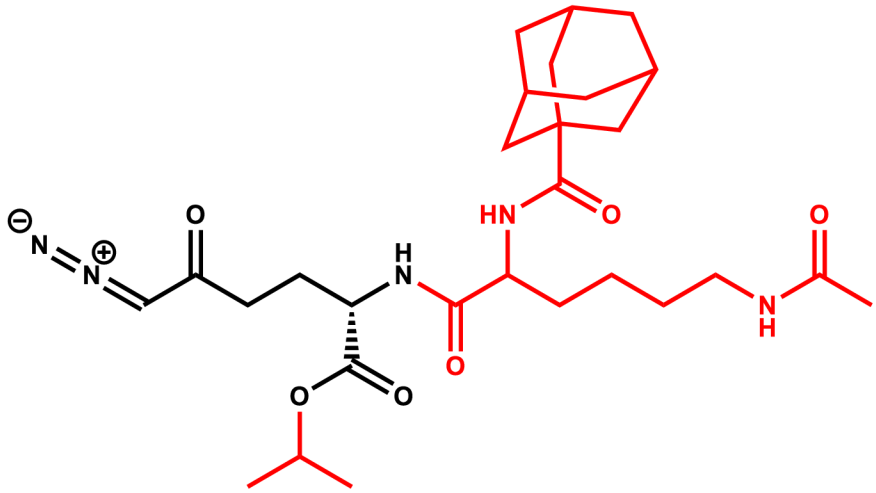

Figure 12: Prodrug 6 (LTP607): the black part represents DON, the red part indicates modifications that increase stability and provide certain specificity toward tumors

2 Aims of the study

- The first objective of the study was to evaluate the compatibility of DON and the DON prodrug (LTP607) with MBTA therapy and to check whether synergy between them can be observed.
- The second objective was to test whether this combination can eliminate secondary tumors (without direct treatment of these tumors).
- The third objective of the study was to analyze and compare the side effects of DON and LTP607.
- Finally, this study aimed to obtain the best possible survival results; therefore, it was essential to analyze how the modification of DON affects (if it does) the survival of mice.

3 Materials and methods

3.1 Materials

Tissue culture medium, mannan isolated from *Saccharomyces cerevisiae*, media supplements, lipoteichoic acid isolated from *Bacillus subtilis*, polyinosinic:polycytidylic acid in the form of sodium salt (poly (I:C)), and 6-diazo-5-oxo-L-norleucine (DON) were purchased from Sigma-Aldrich (St. Louis, MO, USA). The biocompatible anchor for the cell membrane (BAM with a molecular weight of 4000) was manufactured and purchased from NOF EUROPE (Grobbendonk, Belgium). Resiquimod (R-848) was provided by Tocris Bioscience (Bristol, UK). Monoclonal antibody anti-CD40 (rat IgG2a, clone FGK4.5/FGK45) was purchased from BioXCell (West Lebanon, NH, USA). LTP607 was synthesized by Dr. Majer (IOCHB, Prague) [74].

3.2 Cell line and animals

The cell line Panc02 (murine pancreatic adenocarcinoma) was obtained from Prof. Lars Ivo Partecke (Greifswald, Germany). Cells were kept in Dulbecco's modified eagle medium (DMEM) supplemented with 10% heat-inactivated fetal bovine serum and antibiotics (PAA, Pasching, Austria). Cells were cultured at 37 °C in humidified air with 5% CO_2.

Specific pathogen-free C57BL/6 female mice were purchased from Charles River Laboratories (Sulzfeld, Germany). Mice weighing between 18 and 20 g were kept in specific pathogen-free barrier facilities, and sterile food and water were always available; the photoperiod was 12/12.

3.3 Methods

3.3.1 Preparation of chemicals

Synthesis of mannan-BAM:

The preparation has been carried out according to the procedure reported by Caisová et al. [23]. First, the terminal, reducing group of mannan was aminated with a mixture of sodium cyanoborohydride and ammonium acetate at a pH of 7.5 at 50 °C for five days. The solution obtained was purified by dialysis against PBS at 4 °C overnight. After that, the attachment of the BAM group was performed. For that, the N-hydroxysuccinimidyl group of BAM reacted with the amino group of previously aminated mannan (Figure 13).

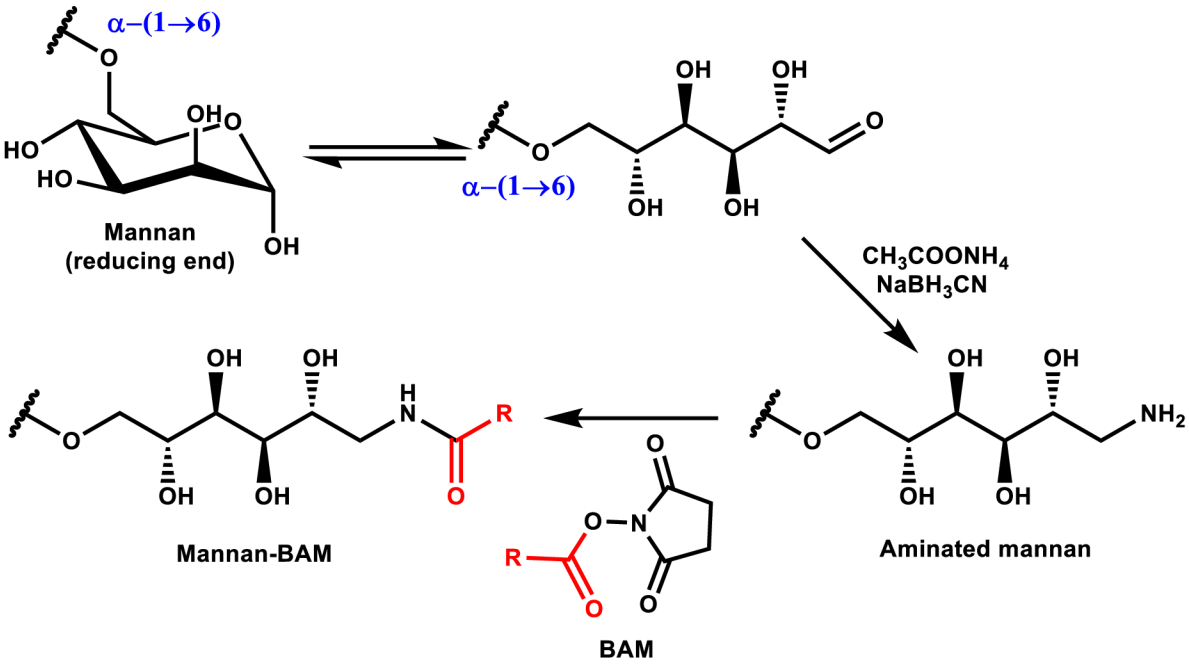

Figure 13: the Mannan-BAM synthesis scheme

MBTA mixture:

25 mg of poly(I:C), 25 mg of LTA, and a solution of resiquimod (prepared from 25 mg of resiquimod and dissolved in the mixture containing 625 µL of PBS and 70 µL of 3.5% HCl) were added to 47 mL of 0.22 mM solution of mannan-BAM in PBS. Hydrochloric acid was added to the solution of the resiquimod in order to increase its solubility in PBS. Additionally, anti-CD40 antibodies were added to the final concentration of 0.4 mg/mL (approximately 2.25 mL).

LTP607 solution:

39.8 mg of LTP607 (Mw = 545.7 g/mol) obtained from the Drug Discovery group (Institute of Organic Chemistry and Biochemistry of the CAB) were dissolved in 6.25 mL of PBS to yield the final concentration of 11.7 mmol/L or 6.37 mg/mL

DON solution:

12.5 mg of DON (171.2 g/mol) were dissolved in 6.25 mL of PBS to yield the final concentration of 11.7 mmol/L or 2 mg/mL

3.3.2 Preparation of mice

C57BL/6 mice (females) were shaved from both sides (flanks), and after that, 400 000 Panc02 cells (murine pancreatic adenocarcinoma cells suspended in 0.1 ml of DMEM) were injected into each side. Two tumors in each mouse represent primary and secondary tumors that can naturally arise. Twelve days later, after incubation, mice were randomly distributed into groups containing six mice in each group. The same day, the first therapy

was applied (day 0). Non-necrotic tumors were primarily chosen because, in this case, the therapeutic agent is less likely to leak out of the tumor.

3.3.3 Treatment and measurements

Treatment has been carried out according to the following scheme:

1) MBTA was applied intratumorally (50 μL) three days in a row, followed by 5-day gaps (starting from day 0).
2) DON and LTP607 were applied intraperitoneally (100 μL) once a week (starting from day 1).
3) The control group was treated with 50 μL of PBS intratumorally, three days in a row, followed by a 5-day gap (starting from day 0).

Seven groups of mice were treated according to the following table:

Table 1: Groups of the experiment and corresponding treatment

Group	Intratumoral application (right tumors)	Intratumoral application (left tumors)	Intraperitoneal application
MBTA/MBTA (**A**)	50 μL MBTA	50 μL MBTA	-
MBTA (**B**)	50 μL MBTA	-	-
MBTA/LTP607 (**C**)	50 all MBTA	-	100 μL LTP607
PBS/LTP607 (**D**)	50 μL PBS	-	100 μL LTP607
MBTA/DON (**E**)	50 μL MBTA	-	100 μL DON
PBS/DON (**F**)	50 μL PBS	-	100 μL DON
PBS (**G**)	50 μL PBS	-	-

Measurements:

The height and length of the tumors were measured in millimeters with an electronic digital caliper. Measurements have been performed for 30 days, each second day starting from day 0. After that, mice were observed for an additional 90 days to obtain survival results (Figure 14).

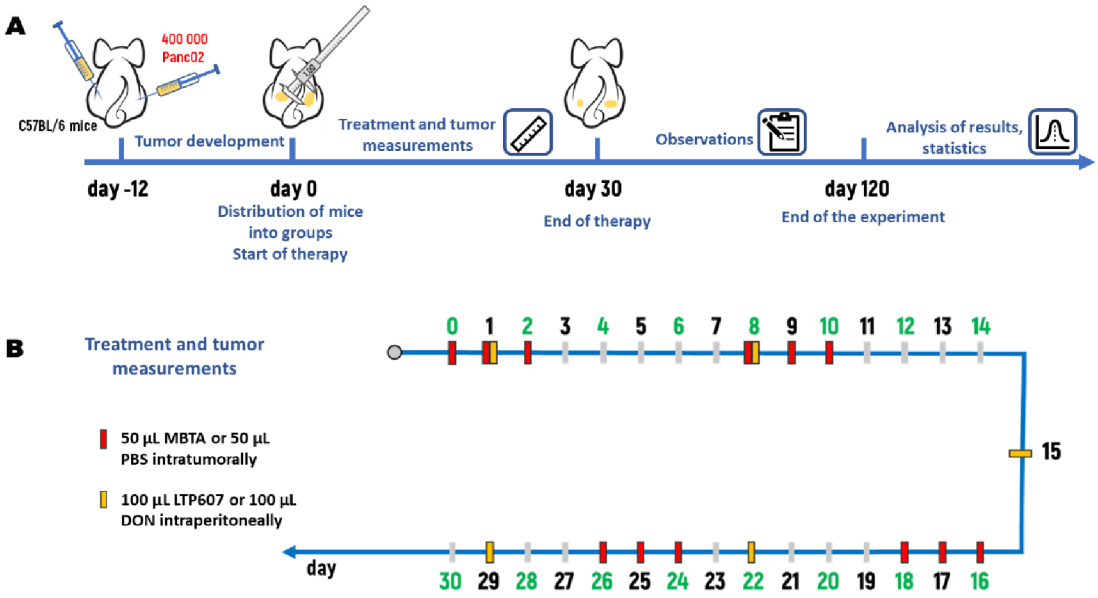

Figure 14: Scheme of the experiment. (**A**) 400 000 Panc02 cells were injected into the right and left flanks of C57BL/6 mice. After 12 days, mice were randomly assigned to 7 groups (6 mice in each group). From day 0 until day 30 treatments and measurements were performed. After that, observations were made for an additional 90 days. Day 120 represents the end of the experiment and the beginning of the analysis of the results obtained. (**B**) The scheme of treatment is shown. MBTA and PBS were applied intratumorally three times in a row with 5-day gaps between (shown as red marks on the timeline), while DON and LTP607 were applied intraperitoneally once a week (shown as yellow marks on the time line). The days shown in green in (**B**) represent the days on which tumor measurements were performed.

3.3.4 Evaluation of results

Tumor volumes have been evaluated according to the following formula [22]:

$$V_i = \frac{1}{6}\,\pi * A_i * B_i^2 \tag{1}$$

where A is the tumor length, while B is the tumor height.

Mean values and standard deviation (SD) have been calculated from the six obtained values (tumor volumes):

$$\bar{V} = \frac{\sum_{i=1}^{n} V_i}{n} \tag{2}$$

$$\sigma = \sqrt{\frac{\sum_{i=1}^{n}(V_i - \bar{V})^2}{n-1}} \tag{3}$$

where $n = 6$, which represents six mice in each group.

Additionally, the standard error of the mean (SEM) has been calculated according to the following formula:

$$SEM = \frac{\sigma}{\sqrt{n}} \tag{4}$$

The error bars on the graphs below represent SEM.

Calculations of the area under the curve (AUC) have been evaluated for mean tumor volume curves. To find the area under the curve, the equation of the function should be known. This can be obtained if the coordinates of two points that lie on the curve are known by the following equation:

$$\frac{y - y_1}{x - x_1} = \frac{y_2 - y_1}{x_2 - x_1} \tag{5}$$

The equation can be rearranged as follows:

$$y = \frac{y_2 - y_1}{x_2 - x_1} * x - \frac{x_1(y_2 - y_1) - y_1(x_2 - x_1)}{x_2 - x_1} \tag{6}$$

Now, the integration with bounds from x_2 to x_1 should be done in order to obtain the function for the area:

$$S = \int_{x_1}^{x_2} y\, dx = \left(\frac{y_2 - y_1}{x_2 - x_1} * x^2 - \frac{x_1(y_2 - y_1) - y_1(x_2 - x_1)}{x_2 - x_1} * x \right) \Bigg|_{x_1}^{x_2}$$

$$S = \frac{y_2 - y_1}{2(x_2 - x_1)} * (x_2^2 - x_1^2) - \frac{x_1(y_2 - y_1) - y_1(x_2 - x_1)}{x_2 - x_1} * (x_2 - x_1)$$

Finally, we obtain the following equation:

$$S = 0.5(x_2 - x_1)(y_2 + y_1) \tag{7}$$

The equation can be further simplified because x values represent the days of therapy, which has been done once in two days so that $x = [0, 2, 4, 6 \ldots]$. Therefore, $x_2 - x_1$ is always equal to 2:

$$S = y_2 + y_1 \tag{8}$$

The equation can be used to calculate the AUC between two days (e.g., day 0 and day 2). The total area is the sum of such pieces (an example is shown in the figure below, where the total AUC between days 0 and 4 is calculated). This way, the AUC has been calculated for each separate mouse (Figure 15). After that, the mean value, standard deviation, and SEM were calculated.

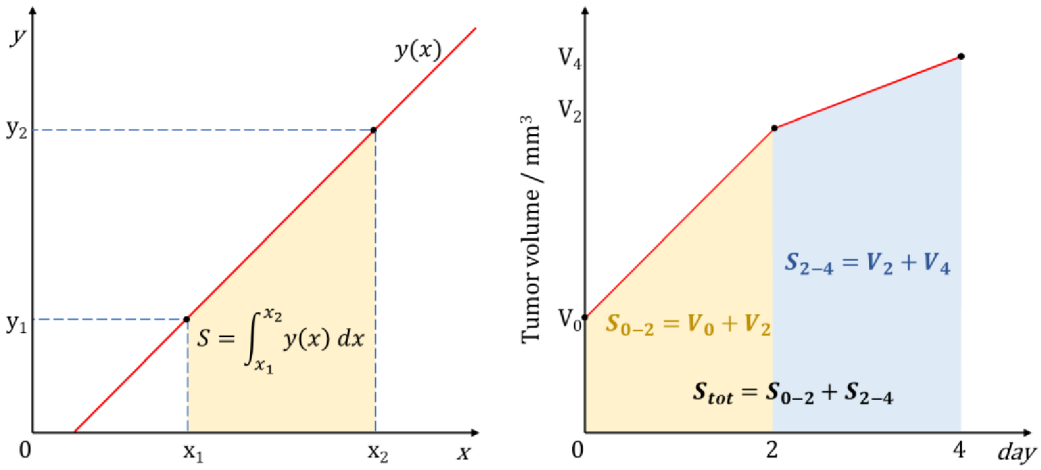

Figure 15: Calculation of AUC: mathematical model (left graph) and its application in the experiment (right picture)

The obtained values for the AUC were analyzed using one-way ANOVA (Tukey's HSD test). However, the test requires homogeneity of variances which has been tested using the Cochran C test. In the cases when the data did not appear homogeneous, log10 was used.

Survival analysis has been presented as Kaplan–Meier curves, and statistical significance has been analyzed using the log-rank test.

Additionally, a paired T-test has been used to test the difference between right and left tumors.

Data were analyzed using STATISTICA 13 software (StatSoft, Inc., Tulsa, OK, USA), and the graphs were plotted in Microsoft Excel.

4 Results

4.1 Analysis of tumor volumes in the course of therapy

Although the measurements were running for 30 days, the results are shown only until day 26 (Figure 16). Due to the death of mice in some groups at the end of therapy, the area under the curve in the case of dead mice cannot be evaluated.

First, a comparison of MBTA used on both sides versus MBTA used only in the right tumors has been made. The experiment showed that when MBTA was applied to both sides (group A), no significant differences between left and right tumors were observed (p-value 0.15825 for group A in the paired T-test), as can be seen from Figure 17. On the other hand, if MBTA is applied only to the right side (group B), then a significant difference is observed between the left and right tumors (p-value 0.00002 for group B in the paired T-test, Figure ***17*** and Figure 25). Furthermore, Tukey's HSD test revealed the statistical difference between group A and group B for the left side (a p-value of 0.0059 was obtained). It is also worth mentioning that, as shown in Figure 19, no significant differences were observed between the group where MBTA was applied to both sides (group A) and the group where MBTA was applied to the right tumor only and combined with LTP607 (group C)

Second, the difference between the combination of MBTA with DON (group E) and LTP607 (group C) was evaluated. Tukey's HSD test did not show statistical differences between these groups (p-values of 0.9984 and 0.9589 for right and left tumors, respectively, Figure 18). However, a significant statistical difference was observed between the right and left tumors in group E but not in group C (p-value of 0.1702 and 0.0008 for group C and E in the paired T-test, respectively).

Finally, the synergy between MBTA and LTP607 was analyzed. As can be seen from Figure 20, there is a significant statistical difference between the groups in which LTP607 was combined with MBTA (group C) and with PBS (group D). Tukey's HSD test resulted in p - values of 0.0145 and 0.0034 for right and left tumors, respectively. In addition, a significant statistical difference in left tumors can be observed when we compare group C and group B (in which MBTA was used alone). A p-value of 0.0025 was obtained in the Tukey HSD test (Figure 21). Furthermore, the volumes of the left tumor in group B (where MBTA has been applied alone) are not statistically different from those of the control group G (p-value is 0.8244 in Tukey's HSD test, Figure 23). In addition, no differences were observed between control group G and the group where LTP607 was combined with PBS

(group D), as can be seen in Figure 22. The synergy of MBTA with LTP607 and MBTA with DON is summarized in Figure 24.

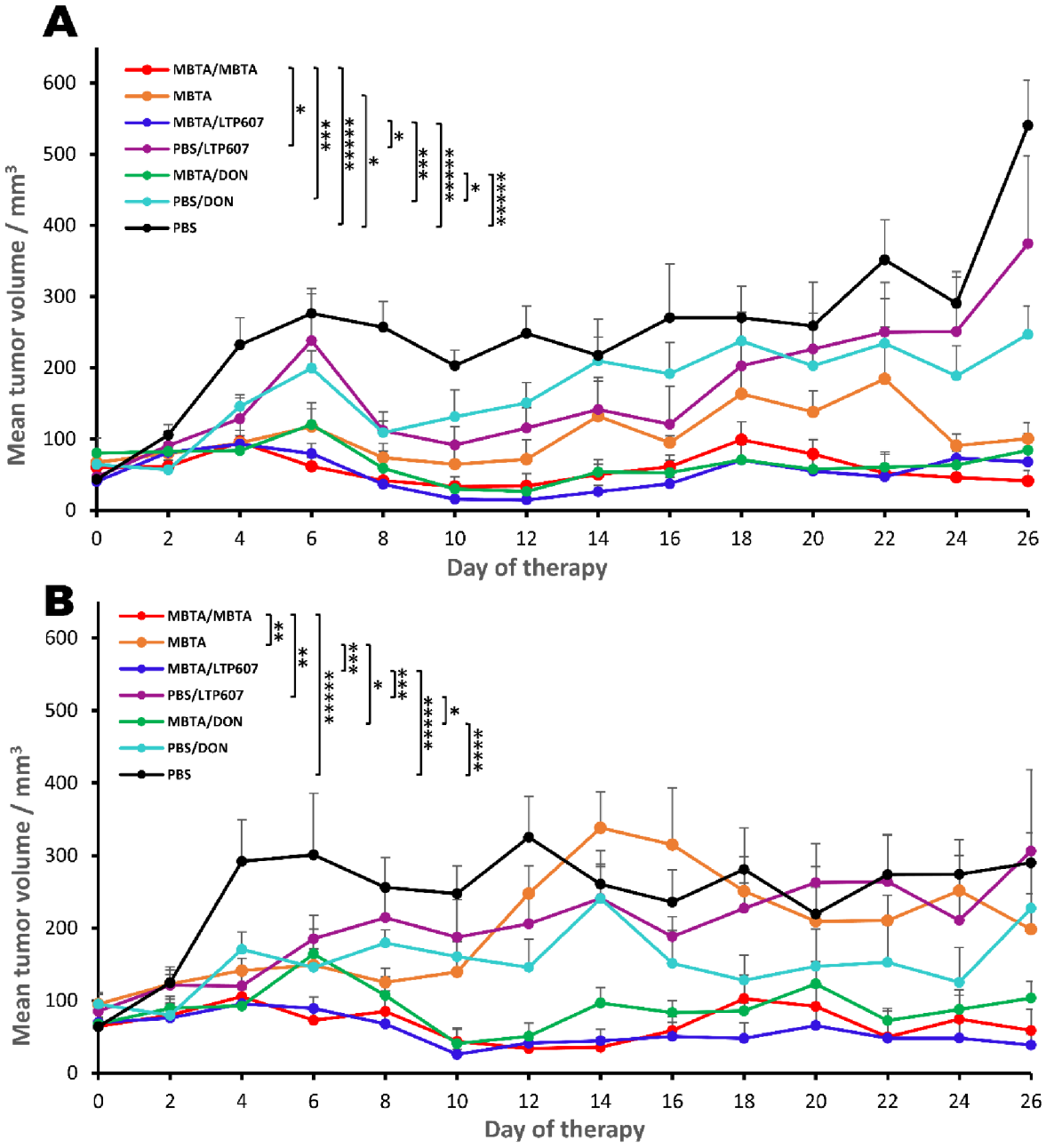

Figure 16: 400 000 Panc02 cells were injected into the right and left flanks of C57BL/6 mice. After 12 days, the mice were randomly assigned to 7 groups (6 mice in each group): MBTA/MBTA (both tumors were treated with MBTA), MBTA (only right tumors were treated with MBTA), MBTA/LTP607 (right tumors were treated with MBTA, LTP607 was used intraperitoneally), PBS/LTP607 (right tumors were treated with PBS, LTP607 was used intraperitoneally), MBTA/DON (right tumors were treated with MBTA, DON was used intraperitoneally), PBS/DON (right tumors were treated with PBS, DON was used intraperitoneally), PBS (right tumors were treated with PBS). The volume of the right tumors (**A**) and the left tumors (**B**) is shown as a growth curve. Tukey's HSD test has been performed (*p≤0.05, **p≤0.01, ***p≤0.005, ****p≤0.001, *****p≤0.0005, ******p≤0.0001).

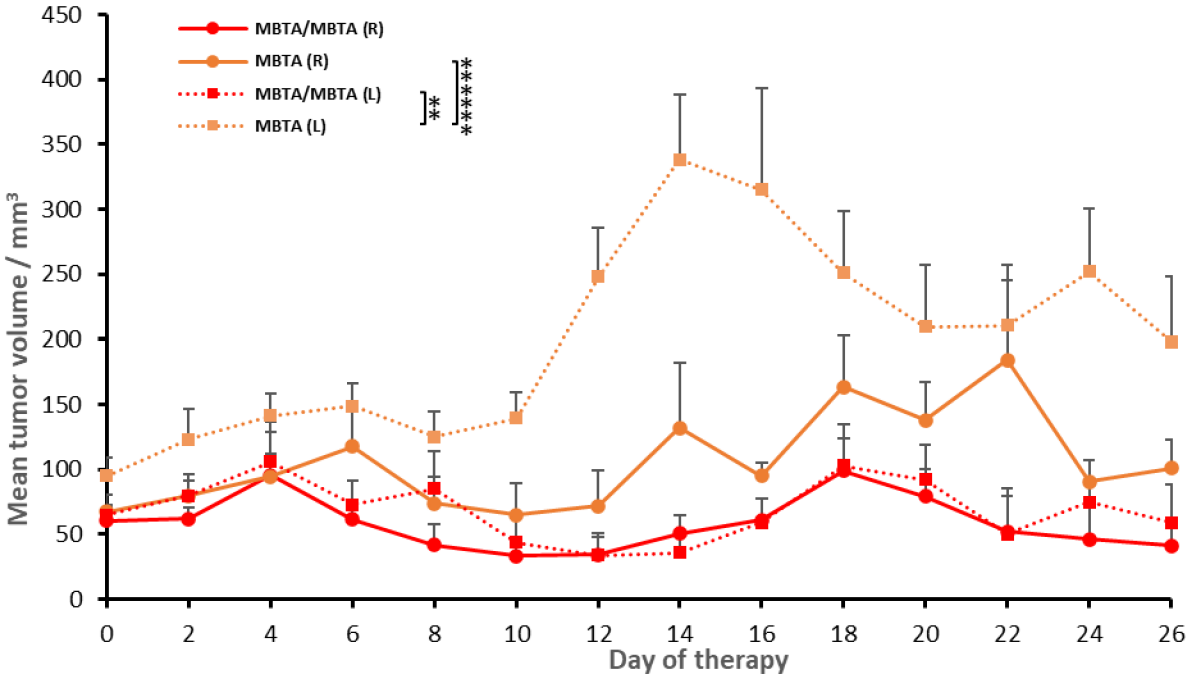

Figure 17: Comparison of MBTA applied to both sides and MBTA applied to the right tumor only. Tukey's HSD test confirmed a significant difference between these groups for both sides (right (R) and left (L)). Moreover, the difference between the right and left tumors can be detected by paired T-test in the group where MBTA was applied only to the right tumors (**p≤0.01, ******p≤0.0001).

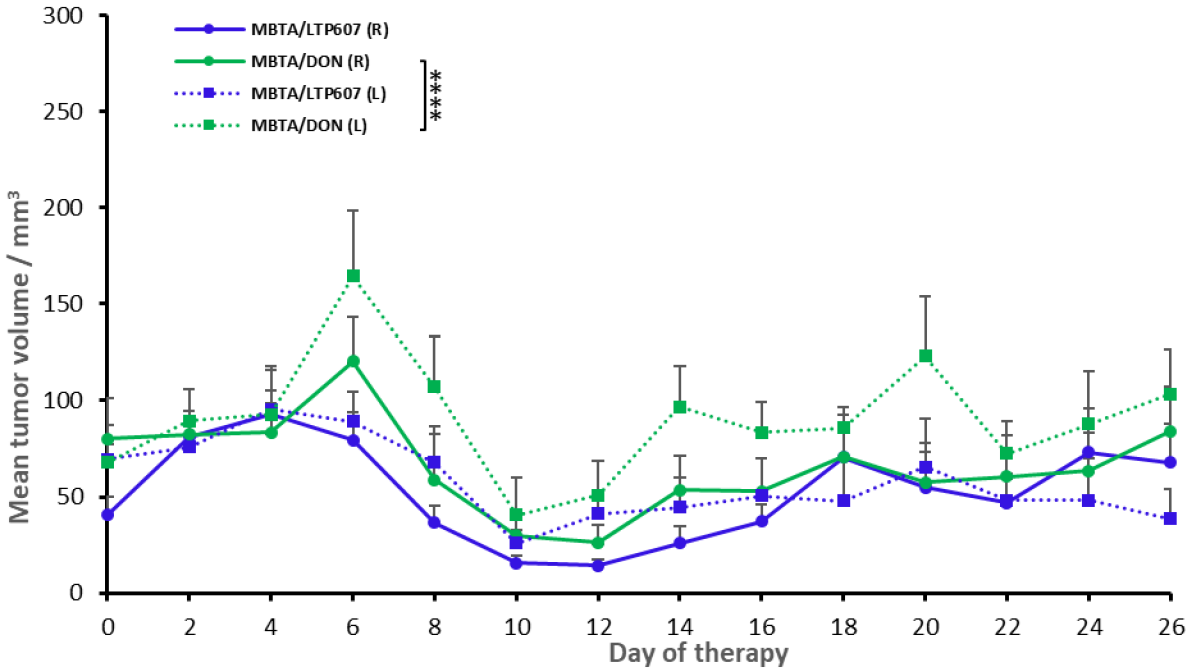

Figure 18: Comparison of MBTA combined with DON and MBTA combined with LTP607. The paired T-test revealed the difference between the right and left tumors in the group where MBTA was combined with DON (****p≤0.001)

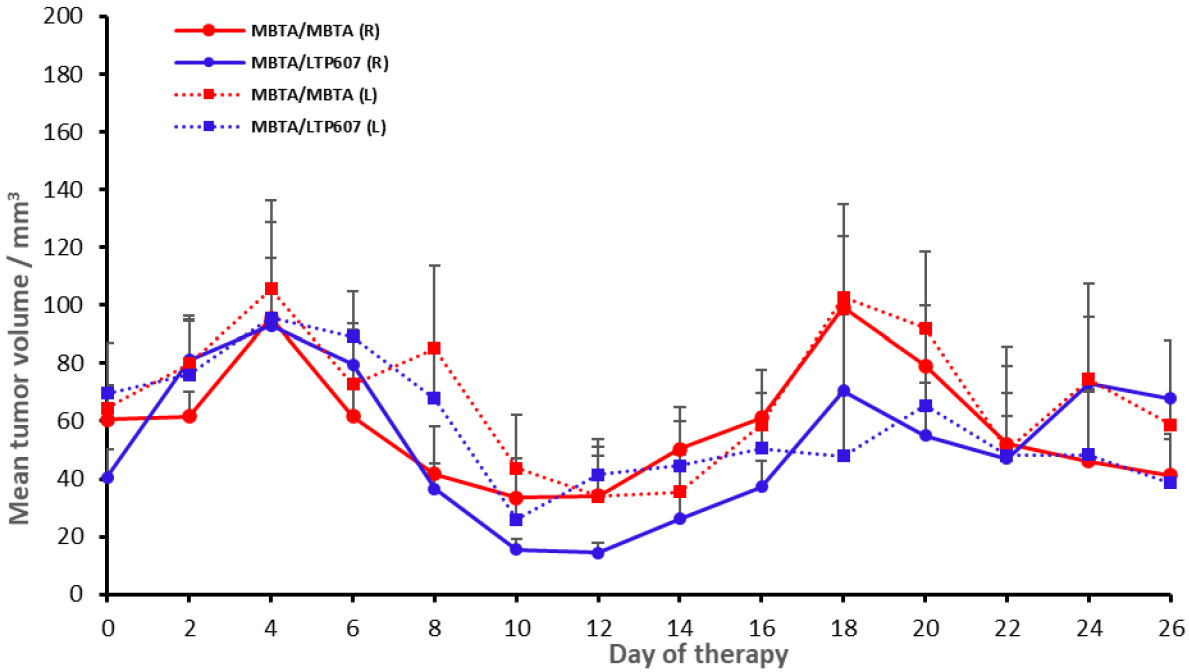

Figure 19: Comparison of MBTA applied to both sides and MBTA applied only to the right side but combined with LTP607. No significant statistical difference in mean tumor volume was confirmed

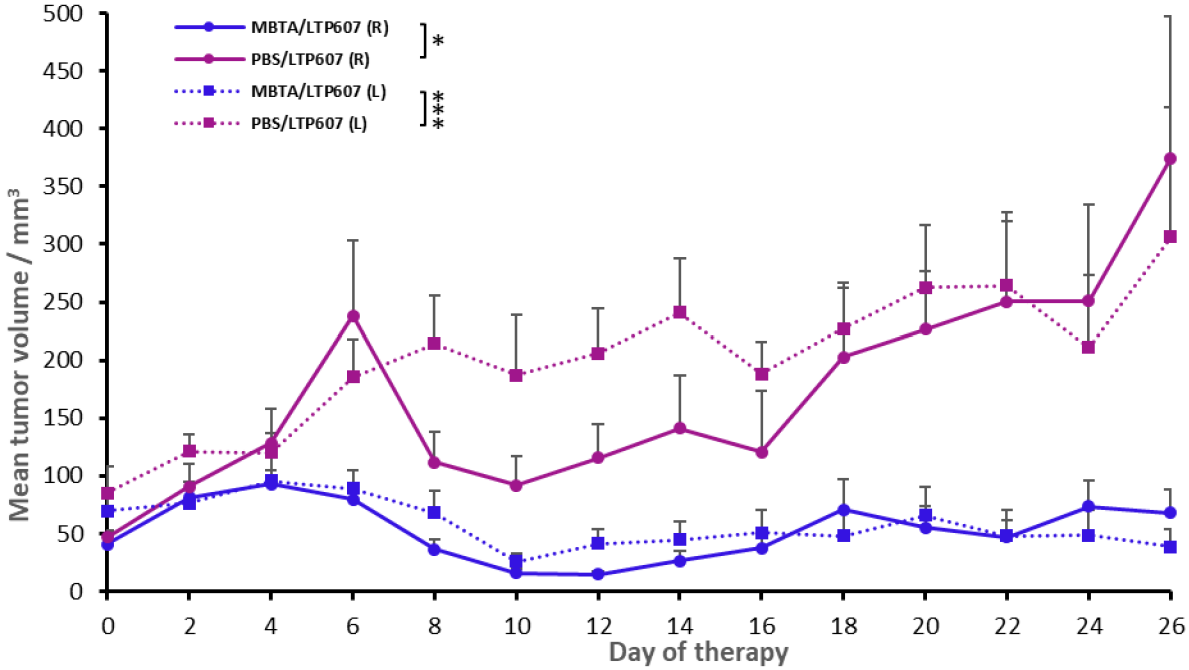

Figure 20: Comparison of MBTA combined with LTP607 and PBS combined with LTP607. Tukey's HSD test confirmed the difference between these groups on the left (L) and right (R) sides (*$p \leq 0.05$, ***$p \leq 0.005$)

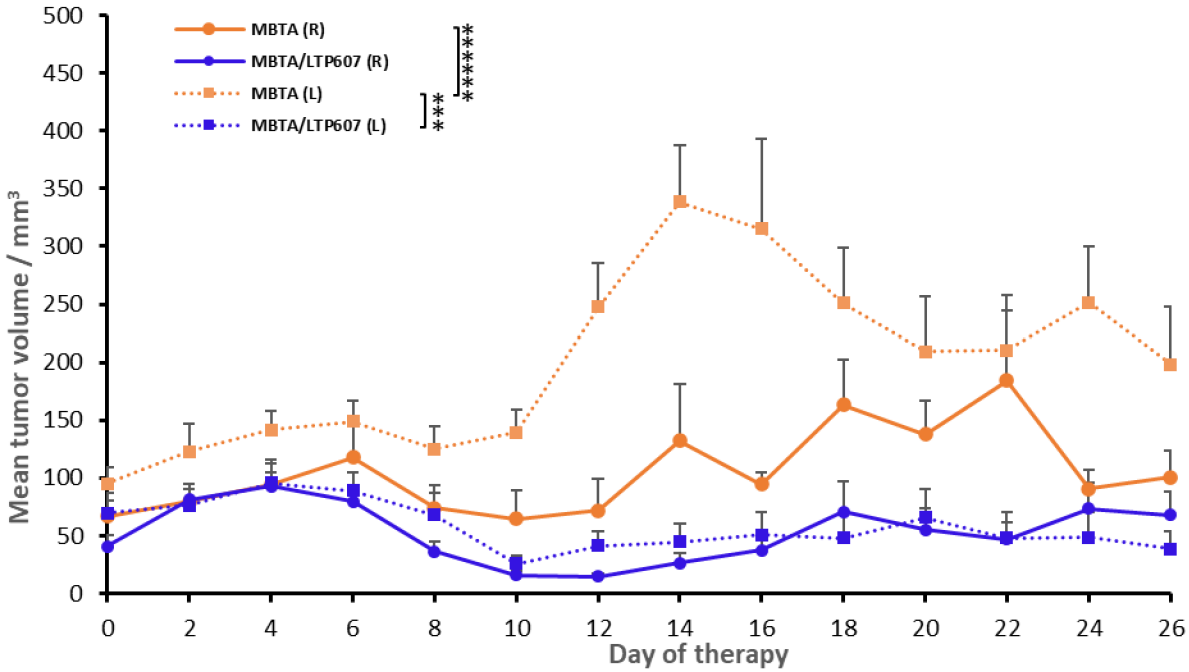

Figure 21: Comparison of MBTA combined with LTP607 and MBTA applied solely to right tumors. Tukey's HSD test revealed the difference in mean tumor volumes for both sides between these groups. Furthermore, the paired T-test shows the difference between left and right tumors in the group where MBTA was applied alone (***p≤0.005, ******p≤0.0001)

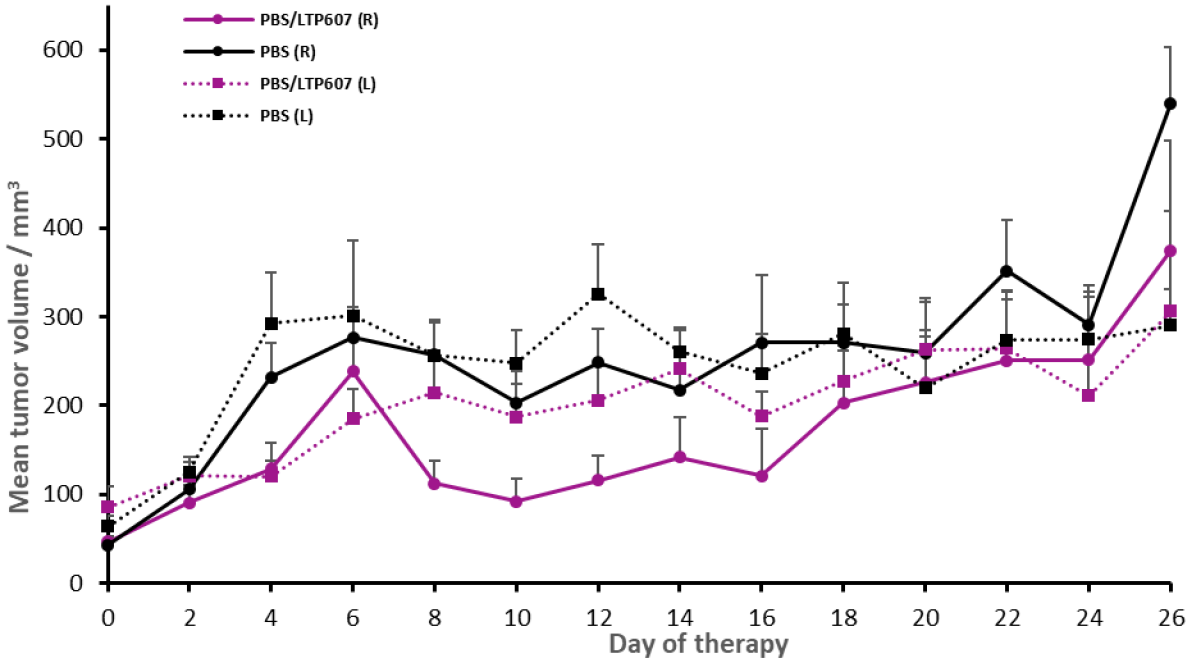

Figure 22: Comparison of PBS and PBS combined with LTP607. No significant difference was detected in mean tumor volume. Therefore, the application of LTP607 alone is not enough to significantly reduce tumor volume.

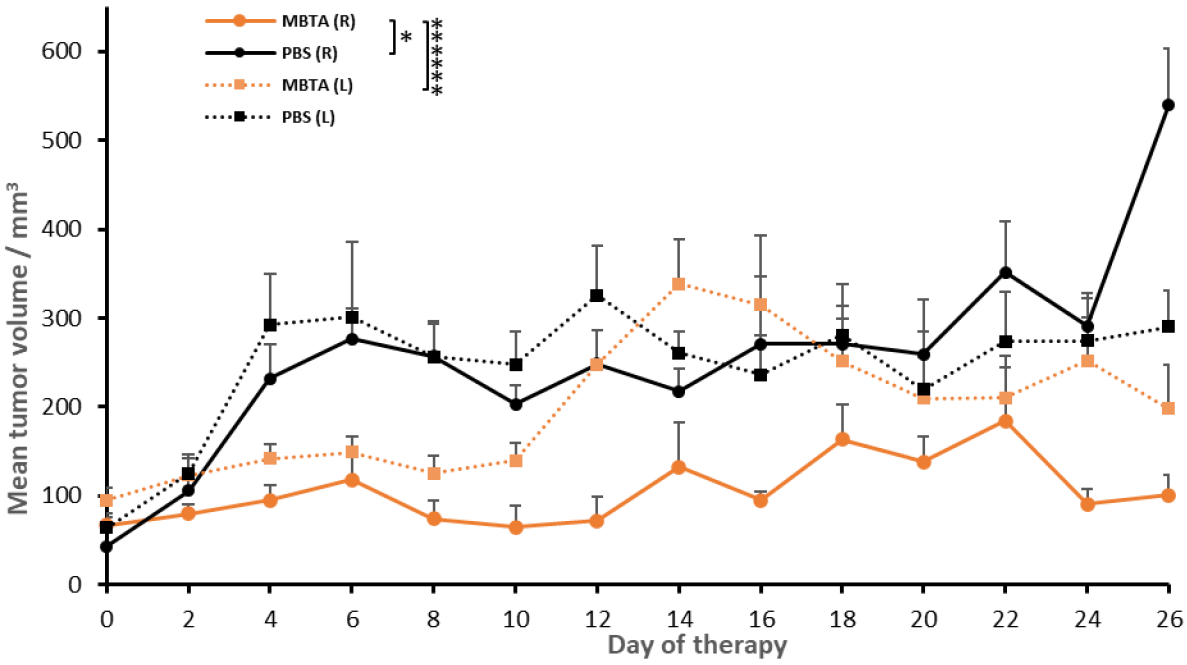

Figure 23: Comparison of MBTA applied only in right tumors and PBS. Tukey's HSD test revealed that a significant difference in mean tumor volume can be observed between the right tumors but not between the left ones. The paired T-test further confirmed this difference between the right and left tumors in the group where MBTA was applied (*p≤0.05, ******p≤0.0001)

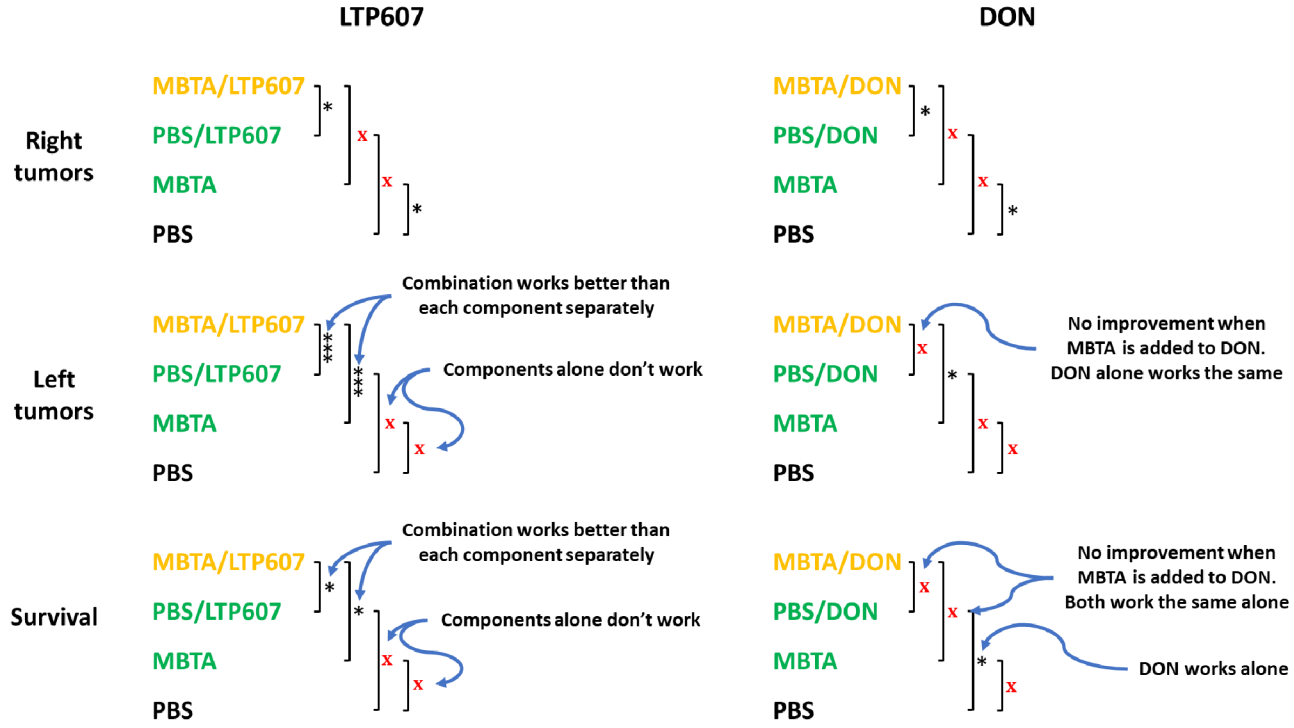

Figure 24: Synergy between MBTA and LTP607 and between MBTA and DON. Yellow color represents the combination of two therapies. Green color represents each therapy which was applied individually. PBS is the control group. The statistical difference between groups represent values obtained from Tukey's HSD test (x means p>0.05 ,*p≤0.05, ***p≤0.005).

4.2 Area under the curve calculations

The AUC has been calculated for each separate mouse. It can be seen from Figure 29 that the variances between the groups are not homogeneous for the right tumors. The difference in variance has been confirmed by the Cochran C test. Therefore, log10 of the data, which resulted in homogeneous variances, was used to calculate Tukey's test.

The values obtained for AUC (in the way demonstrated in Figure 15) were used to calculate relative values (Table 15) with respect to control group G, which constitutes 100%. The obtained values were graphically represented in Figure 25. The best result in volume reduction was obtained for group C, in which MBTA was combined with LTP607. Tumor reduction was 21.2, and 23.3% compared to the control group for right and left tumors, respectively.

Figure 31 (A) demonstrates that right tumors in groups A (where MBTA was applied to both sides) and B (where MBTA was applied only to right tumors) were statistically different from right tumors in the control group (G) already on the 4^{th} of therapy. In addition, we can see that the difference between groups A and B stayed above the threshold of 0.05 and thus was always not significant; however, it is visible that the p-value was steadily decreasing. Something different was obtained for the left tumors in Figure 31 (B). Here we can see that the difference between group A and control is similar to the situation in the right tumors. On the other hand, MBTA was not applied to left tumors in group B, and thus, the p-value between groups A and B was decreasing until it crossed the threshold at day 12. At this point, we observed a significant difference between groups A and B for left tumors. Finally, it can be noticed that the statistical difference between groups B and G did not change monotonically, although the difference was not significant throughout the whole therapy progression.

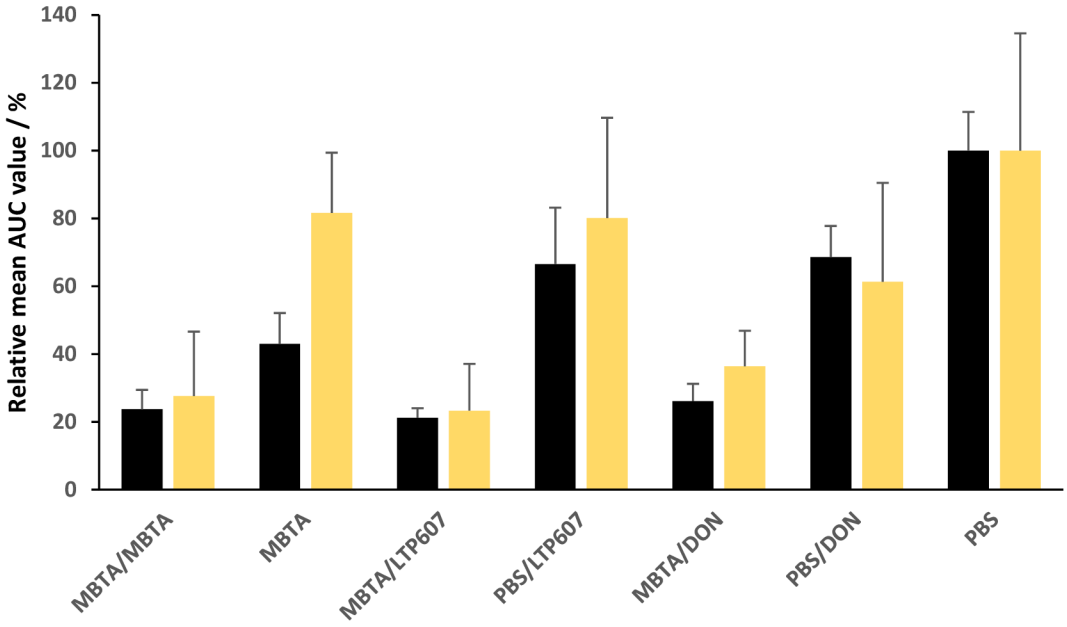

Figure 25: Mean AUC values relative to the control group value (the value obtained for the group where PBS was used is considered to be 100%). Black bars represent right tumors, while yellow bars represent left tumors

4.3 Survival analysis

As can be seen from Table 3, the best survival results were obtained when MBTA was applied to both sides (group A), where the mean lifespan was 98 days. Log-rank test revealed the statistical difference between group A and all other groups (Figure 26) besides groups where MBTA applied to one side was combined with LTP607 (group C) and DON (group E) (p-values 0.3285 and 0.0856 for group C and group E, respectively). In addition, a complete cure was observed only in group A (in which three mice survived till the end of the experiment (120 days)) and in group C (in which one mouse survived, Table 2).

However, if we consider the group where MBTA was applied only to one side (group B), then it was obtained that this group significantly differs from two groups: group A (MBTA applied to both sides) and group C (MBTA combined with LTP607) but no difference was observed with group E where MBTA was combined with DON. The corresponding p-values 0.0242, 0.0288, and 0.0528 were obtained in the Log-rank test when group B was compared to groups A, C, and E, respectively.

In addition, there was not a significant difference between groups B and G (which is the control group), where a p-value of 0.1565 was obtained in the Log-rank test. In a similar way, when LTP607 was combined with PBS (group D), no difference from the

control group was observed (p-value 0.1540). However, a significant difference with the control group was confirmed when DON was combined with PBS (a p-value of 0.0201 was obtained in the Log-rank test).

Table 2: Lifespan of mice in days (120 days is a threshold indicating that the mouse is cured)

Mouse	Lifespan / days	Mouse	Lifespan / days
A1	120	D4	56
A2	71	D5	26
A3	120	D6	59
A4	120	E1	88
A5	56	E2	98
A6	98	E3	70
B1	37	E4	86
B2	61	E5	73
B3	37	E6	49
B4	59	F1	77
B5	40	F2	51
B6	77	F3	88
C1	111	F4	56
C2	94	F5	59
C3	120	F6	53
C4	77	G1	28
C5	65	G2	40
C6	70	G3	45
D1	28	G4	24
D2	70	G5	40
D3	45	G6	53

Table 3: Mean lifespan in days for all groups

		Mean lifespan / days
Group	MBTA/MBTA (A)	98
	MBTA (B)	52
	MBTA/LTP607 (C)	90
	PBS/LTP607 (D)	47
	MBTA/DON (E)	77
	PBS/DON (F)	64
	PBS (G)	38

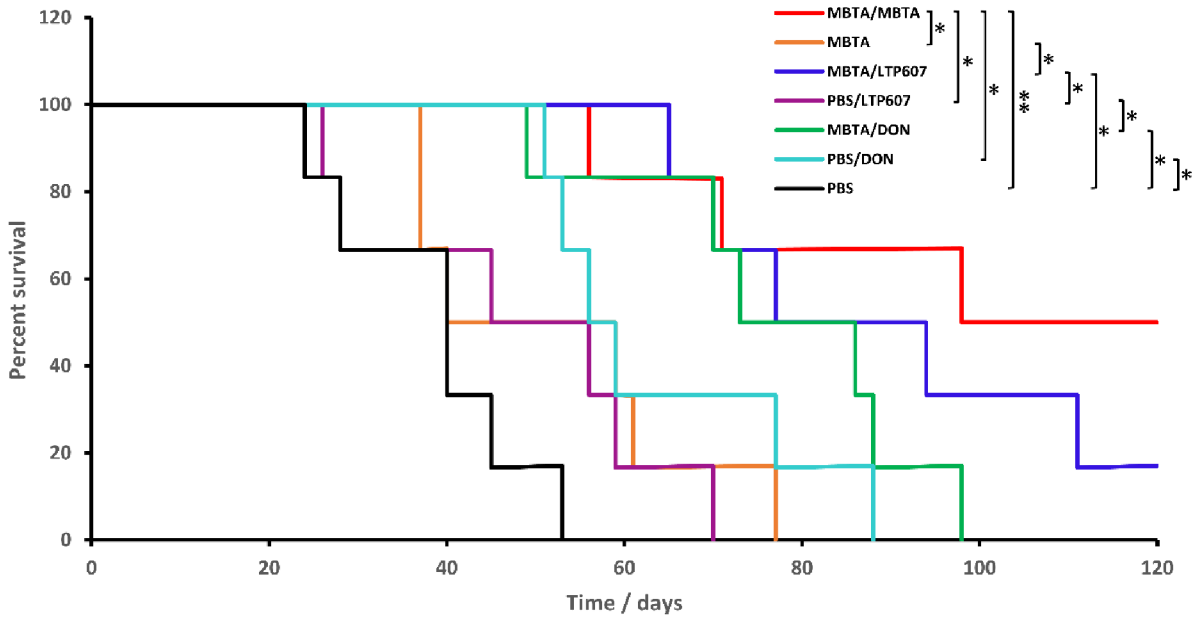

Figure 26: 400 000 Panc02 cells were injected into the right and left flanks of C57BL/6 mice. After 12 days, mice were randomized into seven groups (six mice in each group): MBTA/MBTA (both tumors were treated with MBTA), MBTA (only right tumors were treated with MBTA), MBTA/LTP607 (right tumors were treated with MBTA, LTP607 was used intraperitoneally), PBS/LTP607 (right tumors were treated with PBS, LTP607 was used intraperitoneally), MBTA/DON (right tumors were treated with MBTA, DON was used intraperitoneally), PBS/DON (right tumors were treated with PBS, DON was used intraperitoneally), PBS (right tumors were treated with PBS). The results were shown as Kaplan-Meier curves. Log-rank test has been performed (*p≤0.05, **p≤0.01, ***p≤0.005, ****p≤0.001, *****p≤0.0005, ******p≤0.0001).

5 Discussion

Despite continuous research and progress, pancreatic cancer remains a very challenging type of cancer [65]. Driving by various mutations, this cancer often acquires metastatic and invasive character [65]. Although primary tumors can be found and treated relatively easily, secondary tumors are not always reachable. This is the reason why metastasis is the leading cause of cancer-related deaths [85].

Therefore, the objective of the experiment was to simulate the actual situation and try to cure mice with secondary tumors without direct (intratumoral) treatment of these secondary tumors. It was shown that it was possible to achieve significant tumor reduction on both sides when MBTA was applied to both sides. MBTA applied in this manner showed the best result in terms of mice survival, where the mean lifespan was 98 days from the first day of therapy. Additionally, half of the mice in this group (group A) were completely cured at the end of therapy.

However, MBTA applied to only the right tumors was not sufficient to reduce the volume of the left tumors. These results are totally consistent with the data previously reported by Uher, Caisova et al., who came to the conclusion that MBTA applied alone is not sufficient to eradicate distant secondary tumors [78]. Furthermore, we found that MBTA applied alone is not sufficient to prolong the lifespan of mice significantly.

As mentioned above, the left tumors in group B (MBTA) were different from the left tumors in group A (MBTA/MBTA) at the end of therapy. This makes sense if we consider that the left tumors were treated directly in group A but not in group B. However, the statistical difference between these groups was established only on the 12^{th} day of therapy. Furthermore, the difference between group B and control group (G) began to decrease steadily on day 14. What is the reason behind this phenomenon? It is well known that innate immunity enters into play much earlier than adaptive immunity [6]. Thus, I would assume that the main effect and tumor reduction in group B at the beginning of therapy are explained by TLR ligands which are included in MBTA therapy. It is known that TLR ligands (for example, resiquimod) induce the production of various cytokines [4]. Some of them (such as IL-6 and TNF-α) might act in an endocrine way and thus be responsible for the observed distant effects [61]. On the other hand, mannan-BAM acts as an artificial opsonin and induces complement and phagocytosis. It recruits phagocytes (such as neutrophils) and thus leads to tumor elimination [77]. However, it is unlikely that mannan-BAM can work on distance, and thus, non-treatable tumors (left) most certainly were not opsonized. Thus, tumor reduction was not that effective, and after

some period of time, the reduction of tumors stopped because of possible resistance that could arise to treatment with TLR ligands. It is also worth mentioning that the MBTA administration scheme (3 days in a row with 5-day gaps) is used to decrease the probability of developing TLR resistance [77].

Often, monotherapy is inefficient in cancer therapy, and a more sophisticated approach is required. Thus, one way to improve the effect of treatment is to combine several approaches that act together against cancer [12]. The strategy is often beneficial and results in higher efficiency and reduces the drug resistance effect [12]. Although MBTA therapy is generally not a monotherapy and consists of several active components, its effect can be further improved by combining with other methods that utilize different mechanisms. For example, MBTA was previously shown to be able to be combined with radiotherapy [78].

In this study, we focused on combining MBTA with drugs that broadly inhibit glutamine-utilizing pathways. There are several reasons why exactly glutamine metabolism was chosen as a primary target. It is well known that cancer cells are shown to be glutamine-dependent cells and use them in many pathways that result in the generation of energy, the generation of reducing equivalents, and the biosynthesis of nucleotides [60].

The second reason why we chose this strategy was the data that have been reported to show that inhibition of glutamine metabolism can be successfully combined with immunotherapy. It was previously reported that DON could enhance the therapeutic effect of immunotherapy through several mechanisms [44]. DON not only kills tumor cells, but it also plays a role in changing the tumor microenvironment and thus prevents the development of an immunosuppressive medium [44].

In this thesis, the combination of MBTA with DON and LTP607 (which is the prodrug of DON) was studied. The best result was achieved when MBTA was combined with the intraperitoneal application of LTP607 (group C). In this case, only the right tumors were treated with MBTA, but these right tumors were not significantly different from the left tumors. Furthermore, the group was comparable (no significant difference) with the group where MBTA was applied to both sides in terms of tumor volumes and survival results. The most significant tumor reduction was observed in this group. The combination of MBTA with LTP607 was able to reduce tumors five times compared to the control group. Furthermore, one out of six mice was completely cured and survived until the end of the experiment. It is important to mention that the combination of MBTA with DON (group E) resulted in better results compared to the situation where MBTA was used alone. Survival and tumor reduction

results in group E (MBTA combined with DON) were comparable to group C where MBTA was combined with LTP607. However, in the case of DON (group E), the right tumors were still significantly smaller than the left tumors (which were not treated directly).

Depending on the effect observed, drug combinations can be characterized as synergistic, antagonistic, or additive [62]. Mäkelä et al. describe synergy as the combination of several types of treatments that results in a more significant effect than the sum of each treatment individually [50]. In this study, we observed the synergy between LTP607 and MBTA, which was determined using the Tukey HSD test obtained for left tumors and survival analysis (Log-rank test). In this case, we can say that the combination works better than each component (LTP607 or MBTA) individually. Moreover, the components applied separately did not result in significant differences compared to the control group. Similar observations were detected in the survival results. Neither LTP607 nor MBTA was applied to left tumors, and thus the effect of their combination is possible to detect in left tumors. On the other hand, MBTA was used directly in the right tumors. The combination effect, in this case, is much more difficult to evaluate precisely. This could explain why no difference in right tumors was observed between the group in which MBTA was used alone and the group in which it was combined with LTP607.

However, it is worth mentioning that synergy between DON and MBTA in terms of survival results was not observed. Three groups where MBTA was used alone, DON was used alone, and DON was combined with MBTA were not significantly different from each other. Even being able to increase the lifespan, DON seems to affect immunotherapy, and thus the efficiency of such a combination tends to be not as high.

Although it is beyond the scope of this study to explain why synergy has been observed with LTP607 but not with DON, I would propose that the reason is the higher selectivity of LTP607 toward tumor cells. In turn, selectivity is provided by two enzymes (or at least one enzyme) that are required to liberate DON from its prodrug. MBTA therapy, although it involves many cell types, has been shown to be primarily dependent on two types of immune cells: neutrophils and CD4+ lymphocytes [77, 78]. Although lymphocytes are also considered glutamine-dependent cells [24], there is no strong evidence that $CD4^+$ cells show an increased amount of protease production and, therefore, could not be that susceptible to LTP607.

On the other hand, cathepsin L and other proteases are widely used by cancer cells in the process of invasion, including pancreatic cancer [69]. Furthermore, the adamantyl group

bound to the α-amino group of lysine provides further improved uptake in cells and higher efficacy compared to DON [74].

The higher selectivity of LTP607 versus DON was also observed throughout the experiment in terms of side effects. Some mice treated with DON have severe weight loss and diarrhea. On the other hand, mice treated with LTP607 also suffered weight loss; however, it was less pronounced. As described, DON, to a high degree, affects glutamine-dependent enterocytes that use glutamine for rapid proliferation [37]. This is the main reason for the gastrointestinal toxicity that is very often associated with DON administration [43]. According to Maselli et al., the intestinal epithelium renews every 4-8 days [52]. Thus the chosen application scheme of DON and LTP607 (once per week) is important to reduce the previously mentioned side effects because it allows these cells to recover between application pulses.

Although the synergy between MBTA and LTP607 was confirmed in this study, the molecular basis and mechanism of this effect have yet to be investigated. The elucidation of this mechanism can be a matter of future study. Moreover, a better understanding of the metabolic differences between immune cells (such as lymphocytes, neutrophils, and others) and cancer cells will provide new ways to develop DON prodrugs with even higher selectivity and efficacy. Unfortunately, side effects (even though less severe compared to pure DON itself) are still a key limiting factor. Furthermore, the approach used by HDAC and CTSL to selectively release the prodrug inside tumor cells proved its efficiency and benefits. Other prodrugs that use the same liberating mechanism could be used in the future.

6 Conclusion

The main goals of this thesis were to investigate the compatibility of DON and its prodrug with MBTA immunotherapy, to analyze the synergy between them, to estimate how this combination approach affects the survival result, and to test whether it will be possible to treat secondary tumors like that (without direct intratumoral injections). MBTA was successfully combined with glutamine metabolism inhibitors such as LTP607 and DON, and this combination can result in a higher tumor volume reduction and a longer life span of mice. Moreover, the synergy between LTP607 and MBTA was determined. Combination with LTP607 allowed us to significantly reduce the volume of non-treatable left tumors that can be considered secondary. We also observed that LTP607 works better than DON in terms of survival results, as its action is more selective to tumor cells and results in fewer side effects. In addition, we discovered that individual application of DON or LTP607 is insufficient to eliminate tumors and prolong life, and thus it must be combined with other approaches, such as MBTA immunotherapy. Finally, side effects observed in the case of LTP607 indicate that further research aiming for the higher selectivity of DON is yet to be done.

7 List of abbreviations

ADCC	Antibody-dependent cell-mediated cytotoxicity
α-KG	Alpha-ketoglutarate
BAM	Biocompatible Anchor for Cell Membrane
BCR	B-cell receptor
CDC	Complement-dependent cytotoxicity
cDC1	Conventional type 1 dendritic cell
CLR	C-type lectin receptor
CRP	Complement regulator protein
CTSL	Cathepsin L
DAMP	Damage associated molecular pattern
DC	dendritic cell
DON	6-diazo-5-oxo-L-norleucine
dsRNA	double-stranded RNA
FB	Factor B
FD	Factor D
FI	Factor I
FH	Factor H
FLT3L	Fms-like tyrosine kinase 3 ligand
fMLF	Formyl-methionyl-leucyl-phenylalanine
GI	Gastrointestinal
GLS	Glutaminase
GLUD	Glutamate dehydrogenase
HDAC	Histone deacetylase
IFN	Interferon
Ig	Immunoglobulin
IκB	Inhibitor of nuclear factor kappa B
IKK	IκB-kinase
IRAK	IL-1R-associated kinase
LRR	Leucine rich repeat
LTA	Lipoteichoic acid
mAb	Monoclonal antibody

MAC	Membrane attack complex
MAP	Mitogen-activated protein
MASP	MBL-associated serine proteases
MBL	Mannose-binding lectin
MBTA	Mannan-BAM, TLR Ligands, Anti-CD40 Antibody
MDSC	Myeloid-derived suppressor cell
MHC	Major histocompatibility complex
MyD88	Myeloid differentiation primary response protein 88
NLRs	NOD-like receptors
PAMP	Pathogen-associated molecular pattern
PML	Polymorphonuclear leukocytes
Poly(I:C)	Polyinosinic-polycytidylic acid
PRR	Pattern recognition receptor
PSGL-1	P-selectin glycoprotein-1
RLR	RIG-I-like receptor
ROS	Reactive oxygen species
SP	Serine protease
ssRNA	single-stranded RNA
TAB1	TAK1-binding protein 1
TAK1	TGF-β-activated kinase 1
TCR	T-cell receptor
TED	Thioester domain
TGF-β	Transforming growth factor β
TIR	Toll/IL-1R
TLR	Toll-like receptor
TME	Tumor microenvironment
TNF	Tumor-necrosis factor
TRAF6	TNF-receptor-associated factor 6
UBC13	Ubiquitin-conjugating enzyme 13
UEV1A	ubiquitin-conjugating enzyme E2 variant 1

8 References

[1] Abbott, M. and Ustoyev, Y. 2019. Cancer and the Immune System: The History and Background of Immunotherapy. *Seminars in oncology nursing* 35, 5, 150923.

[2] Adams, J. M. and Cory, S. 2007. The Bcl-2 apoptotic switch in cancer development and therapy. *Oncogene* 26, 9, 1324–1337.

[3] Afshar-Kharghan, V. 2017. The role of the complement system in cancer. *The Journal of clinical investigation* 127, 3, 780–789.

[4] Ahonen, C. L., Gibson, S. J., Smith, R. M., Pederson, L. K., Lindh, J. M., Tomai, M. A., and Vasilakos, J. P. 1999. Dendritic cell maturation and subsequent enhanced T-cell stimulation induced with the novel synthetic immune response modifier R-848. *Cellular immunology* 197, 1, 62–72.

[5] Akira, S. and Takeda, K. 2004. Toll-like receptor signalling. *Nature reviews. Immunology* 4, 7, 499–511.

[6] Alberts, B. 2015. *Molecular biology of the cell*. Garland Science Taylor and Francis Group, New York NY.

[7] Altman, B. J., Stine, Z. E., and Dang, C. V. 2016. From Krebs to clinic: glutamine metabolism to cancer therapy. *Nature reviews. Cancer* 16, 10, 619–634.

[8] Anfray, C., Mainini, F., Digifico, E., Maeda, A., Sironi, M., Erreni, M., Anselmo, A., Ummarino, A., Gandoy, S., Expósito, F., Redrado, M., Serrano, D., Calvo, A., Martens, M., Bravo, S., Mantovani, A., Allavena, P., and Andón, F. T. 2021. Intratumoral combination therapy with poly(I:C) and resiquimod synergistically triggers tumor-associated macrophages for effective systemic antitumoral immunity. *Journal for immunotherapy of cancer* 9, 9.

[9] Banchereau, J. and Steinman, R. M. 1998. Dendritic cells and the control of immunity. *Nature* 392, 6673, 245–252.

[10] Bansal, A. and Simon, M. C. 2018. Glutathione metabolism in cancer progression and treatment resistance. *The Journal of cell biology* 217, 7, 2291–2298.

[11] Bareke, H. and Akbuga, J. 2018. Complement system's role in cancer and its therapeutic potential in ovarian cancer. *Scandinavian journal of immunology* 88, 1, e12672.

[12] Bayat Mokhtari, R., Homayouni, T. S., Baluch, N., Morgatskaya, E., Kumar, S., Das, B., and Yeger, H. 2017. Combination therapy in combating cancer. *Oncotarget* 8, 23, 38022–38043.

[13] Bayly-Jones, C., Bubeck, D., and Dunstone, M. A. 2017. The mystery behind membrane insertion: a review of the complement membrane attack complex. *Philosophical transactions of the Royal Society of London. Series B, Biological sciences* 372, 1726.

[14] Beutler, B. 2004. Innate immunity: an overview. *Molecular immunology* 40, 12, 845–859.

[15] Blasco, M. A. 2005. Telomeres and human disease: ageing, cancer and beyond. *Nature reviews. Genetics* 6, 8, 611–622.

[16] Bohlson, S. S., Fraser, D. A., and Tenner, A. J. 2007. Complement proteins C1q and MBL are pattern recognition molecules that signal immediate and long-term protective immune functions. *Molecular immunology* 44, 1-3, 33–43.

[17] Bonilla, F. A. and Oettgen, H. C. 2010. Adaptive immunity. *The Journal of allergy and clinical immunology* 125, 2 Suppl 2, S33-40.

[18] Böttcher, J. P., Bonavita, E., Chakravarty, P., Blees, H., Cabeza-Cabrerizo, M., Sammicheli, S., Rogers, N. C., Sahai, E., Zelenay, S., and Reis e Sousa, C. 2018. NK

Cells Stimulate Recruitment of cDC1 into the Tumor Microenvironment Promoting Cancer Immune Control. *Cell* 172, 5, 1022-1037.e14.

[19] Böttcher, J. P. and Reis e Sousa, C. 2018. The Role of Type 1 Conventional Dendritic Cells in Cancer Immunity. *Trends in cancer* 4, 11, 784–792.

[20] Broz, M. L., Binnewies, M., Boldajipour, B., Nelson, A. E., Pollack, J. L., Erle, D. J., Barczak, A., Rosenblum, M. D., Daud, A., Barber, D. L., Amigorena, S., Van't Veer, L. J., Sperling, A. I., Wolf, D. M., and Krummel, M. F. 2014. Dissecting the tumor myeloid compartment reveals rare activating antigen-presenting cells critical for T cell immunity. *Cancer cell* 26, 5, 638–652.

[21] Bubeck, D. 2014. The making of a macromolecular machine: assembly of the membrane attack complex. *Biochemistry* 53, 12, 1908–1915.

[22] Caisová, V., Uher, O., Nedbalová, P., Jochmanová, I., Kvardová, K., Masáková, K., Krejčová, G., Paďouková, L., Chmelař, J., Kopecký, J., and Ženka, J. 2018. Effective cancer immunotherapy based on combination of TLR agonists with stimulation of phagocytosis. *International immunopharmacology* 59, 86–96.

[23] Caisová, V., Vieru, A., Kumžáková, Z., Glaserová, S., Husníková, H., Vácová, N., Krejčová, G., Paďouková, L., Jochmanová, I., Wolf, K. I., Chmelař, J., Kopecký, J., and Ženka, J. 2016. Innate immunity based cancer immunotherapy: B16-F10 murine melanoma model. *BMC cancer* 16, 1, 940.

[24] Carr, E. L., Kelman, A., Wu, G. S., Gopaul, R., Senkevitch, E., Aghvanyan, A., Turay, A. M., and Frauwirth, K. A. 2010. Glutamine uptake and metabolism are coordinately regulated by ERK/MAPK during T lymphocyte activation. *Journal of immunology (Baltimore, Md. : 1950)* 185, 2, 1037–1044.

[25] Cavallaro, U. and Christofori, G. 2004. Cell adhesion and signalling by cadherins and Ig-CAMs in cancer. *Nature reviews. Cancer* 4, 2, 118–132.

[26] Chaplin, D. D. 2010. Overview of the Immune Response. *The Journal of allergy and clinical immunology* 125, 2 Suppl 2, S3-23.

[27] Chavakis, E., Choi, E. Y., and Chavakis, T. 2009. Novel aspects in the regulation of the leukocyte adhesion cascade. *Thrombosis and haemostasis* 102, 2, 191–197.

[28] Da Gama Duarte, J., Peyper, J. M., and Blackburn, J. M. 2018. B cells and antibody production in melanoma. *Mammalian genome : official journal of the International Mammalian Genome Society* 29, 11-12, 790–805.

[29] Dahlgren, C. and Karlsson, A. 1999. Respiratory burst in human neutrophils. *Journal of Immunological Methods* 232, 1-2, 3–14.

[30] Di Gaetano, N., Cittera, E., Nota, R., Vecchi, A., Grieco, V., Scanziani, E., Botto, M., Introna, M., and Golay, J. 2003. Complement activation determines the therapeutic activity of rituximab in vivo. *Journal of immunology (Baltimore, Md. : 1950)* 171, 3, 1581–1587.

[31] Dunne, A. and O'Neill, L. A. J. 2003. The interleukin-1 receptor/Toll-like receptor superfamily: signal transduction during inflammation and host defense. *Science's STKE : signal transduction knowledge environment* 2003, 171, re3.

[32] French, R. R., Chan, H. T., Tutt, A. L., and Glennie, M. J. 1999. CD40 antibody evokes a cytotoxic T-cell response that eradicates lymphoma and bypasses T-cell help. *Nature medicine* 5, 5, 548–553.

[33] Gál, P. and Ambrus, G. 2001. Structure and function of complement activating enzyme complexes: C1 and MBL-MASPs. *Current protein & peptide science* 2, 1, 43–59.

[34] Ghai, R., Waters, P., Roumenina, L. T., Gadjeva, M., Kojouharova, M. S., Reid, K. B. M., Sim, R. B., and Kishore, U. 2007. C1q and its growing family. *Immunobiology* 212, 4-5, 253–266.

[35] Guo, R.-F. and Ward, P. A. 2005. Role of C5a in inflammatory responses. *Annual review of immunology* 23, 821–852.

[36] Hanahan, D. and Weinberg, R. A. 2011. Hallmarks of cancer: the next generation. *Cell* 144, 5, 646–674.

[37] Kao, C., Hsu, J., Bandi, V., and Jahoor, F. 2013. Alterations in glutamine metabolism and its conversion to citrulline in sepsis. *American journal of physiology. Endocrinology and metabolism* 304, 12, E1359-64.

[38] Kishore, U., Ghai, R., Greenhough, T. J., Shrive, A. K., Bonifati, D. M., Gadjeva, M. G., Waters, P., Kojouharova, M. S., Chakraborty, T., and Agrawal, A. 2004. Structural and functional anatomy of the globular domain of complement protein C1q. *Immunology letters* 95, 2, 113–128.

[39] Kobie, J. J., Wu, R. S., Kurt, R. A., Lou, S., Adelman, M. K., Whitesell, L. J., Ramanathapuram, L. V., Arteaga, C. L., and Akporiaye, E. T. 2003. Transforming growth factor beta inhibits the antigen-presenting functions and antitumor activity of dendritic cell vaccines. *Cancer research* 63, 8, 1860–1864.

[40] Koppula, P., Zhuang, L., and Gan, B. 2021. Cystine transporter SLC7A11/xCT in cancer: ferroptosis, nutrient dependency, and cancer therapy. *Protein & cell* 12, 8, 599–620.

[41] Kumar, B. V., Connors, T. J., and Farber, D. L. 2018. Human T Cell Development, Localization, and Function throughout Life. *Immunity* 48, 2, 202–213.

[42] Lane, A. N. and Fan, T. W.-M. 2015. Regulation of mammalian nucleotide metabolism and biosynthesis. *Nucleic acids research* 43, 4, 2466–2485.

[43] Lemberg, K. M., Vornov, J. J., Rais, R., and Slusher, B. S. 2018. We're Not "DON" Yet: Optimal Dosing and Prodrug Delivery of 6-Diazo-5-oxo-L-norleucine. *Molecular cancer therapeutics* 17, 9, 1824–1832.

[44] Leone, R. D., Zhao, L., Englert, J. M., Sun, I.-M., Oh, M.-H., Sun, I.-H., Arwood, M. L., Bettencourt, I. A., Patel, C. H., Wen, J., Tam, A., Blosser, R. L., Prchalova, E., Alt, J., Rais, R., Slusher, B. S., and Powell, J. D. 2019. Glutamine blockade induces divergent metabolic programs to overcome tumor immune evasion. *Science (New York, N.Y.)* 366, 6468, 1013–1021.

[45] Li, K., Gor, J., and Perkins, S. J. 2010. Self-association and domain rearrangements between complement C3 and C3u provide insight into the activation mechanism of C3. *The Biochemical journal* 431, 1, 63–72.

[46] Li, Q. and Verma, I. M. 2002. NF-kappaB regulation in the immune system. *Nature reviews. Immunology* 2, 10, 725–734.

[47] Liu, Y., Wu, Q., Wu, X., Algharib, S. A., Gong, F., Hu, J., Luo, W., Zhou, M., Pan, Y., Yan, Y., and Wang, Y. 2021. Structure, preparation, modification, and bioactivities of β-glucan and mannan from yeast cell wall: A review. *International journal of biological macromolecules* 173, 445–456.

[48] Lookian, P. P., Zhao, D., Medina, R., Wang, H., Zenka, J., Gilbert, M. R., Pacak, K., and Zhuang, Z. 2021. Mannan-BAM, TLR Ligands, Anti-CD40 Antibody (MBTA) Vaccine Immunotherapy: A Review of Current Evidence and Applications in Glioblastoma. *International journal of molecular sciences* 22, 7.

[49] Lu, J. and Kishore, U. 2017. C1 Complex: An Adaptable Proteolytic Module for Complement and Non-Complement Functions. *Frontiers in immunology* 8, 592.

[50] Mäkelä, P., Zhang, S. M., and Rudd, S. G. 2021. Drug synergy scoring using minimal dose response matrices. *BMC research notes* 14, 1, 27.
[51] Marshall, J. S., Warrington, R., Watson, W., and Kim, H. L. 2018. An introduction to immunology and immunopathology. *Allergy, asthma, and clinical immunology : official journal of the Canadian Society of Allergy and Clinical Immunology* 14, Suppl 2, 49.
[52] Maselli, K. M., Schlieve, C. R., Frey, M. R., and Grikscheit, T. C. 2020. Stem and progenitor cells of the gastrointestinal tract: applications for tissue engineering the intestine. In *Principles of Tissue Engineering*. Elsevier, 709–721. DOI=10.1016/B978-0-12-818422-6.00039-3.
[53] Masisi, B. K., El Ansari, R., Alfarsi, L., Rakha, E. A., Green, A. R., and Craze, M. L. 2020. The role of glutaminase in cancer. *Histopathology* 76, 4, 498–508.
[54] McEver, R. P. 2002. Selectins: lectins that initiate cell adhesion under flow. *Current Opinion in Cell Biology* 14, 5, 581–586.
[55] McKernan, D. P. 2020. Pattern recognition receptors as potential drug targets in inflammatory disorders. *Advances in protein chemistry and structural biology* 119, 65–109.
[56] Medzhitov, R. 2008. Origin and physiological roles of inflammation. *Nature* 454, 7203, 428–435.
[57] Merle, N. S., Church, S. E., Fremeaux-Bacchi, V., and Roumenina, L. T. 2015. Complement System Part I - Molecular Mechanisms of Activation and Regulation. *Frontiers in immunology* 6, 262.
[58] Merle, N. S., Noe, R., Halbwachs-Mecarelli, L., Fremeaux-Bacchi, V., and Roumenina, L. T. 2015. Complement System Part II: Role in Immunity. *Frontiers in immunology* 6, 257.
[59] Naran, K., Nundalall, T., Chetty, S., and Barth, S. 2018. Principles of Immunotherapy: Implications for Treatment Strategies in Cancer and Infectious Diseases. *Frontiers in microbiology* 9, 3158.
[60] Nguyen, T.-L. and Durán, R. V. 2018. Glutamine metabolism in cancer therapy. *CDR*.
[61] Papanicolaou, D. A. and Vgontzas, A. N. 2000. Interleukin-6: the endocrine cytokine. *The Journal of clinical endocrinology and metabolism* 85, 3, 1331–1333.
[62] Pemovska, T., Bigenzahn, J. W., and Superti-Furga, G. 2018. Recent advances in combinatorial drug screening and synergy scoring. *Current opinion in pharmacology* 42, 102–110.
[63] Pio, R., Ajona, D., and Lambris, J. D. 2013. Complement inhibition in cancer therapy. *Seminars in immunology* 25, 1, 54–64.
[64] Reis, E. S., Mastellos, D. C., Ricklin, D., Mantovani, A., and Lambris, J. D. 2018. Complement in cancer: untangling an intricate relationship. *Nature reviews. Immunology* 18, 1, 5–18.
[65] Ren, B., Cui, M., Yang, G., Wang, H., Feng, M., You, L., and Zhao, Y. 2018. Tumor microenvironment participates in metastasis of pancreatic cancer. *Molecular cancer* 17, 1, 108.
[66] Rosales, C. 2018. Neutrophil: A Cell with Many Roles in Inflammation or Several Cell Types? *Frontiers in physiology* 9, 113.
[67] Satsu, H. 2017. Molecular and cellular studies on the absorption, function, and safety of food components in intestinal epithelial cells. *Bioscience, biotechnology, and biochemistry* 81, 3, 419–425.

[68] Scalise, M., Pochini, L., Console, L., Losso, M. A., and Indiveri, C. 2018. The Human SLC1A5 (ASCT2) Amino Acid Transporter: From Function to Structure and Role in Cell Biology. *Frontiers in cell and developmental biology* 6, 96.

[69] Singh, N., Das, P., Gupta, S., Sachdev, V., Srivasatava, S., Datta Gupta, S., Pandey, R. M., Sahni, P., Chauhan, S. S., and Saraya, A. 2014. Plasma cathepsin L: a prognostic marker for pancreatic cancer. *World journal of gastroenterology* 20, 46, 17532–17540.

[70] Sionov, R. V., Fridlender, Z. G., and Granot, Z. 2015. The Multifaceted Roles Neutrophils Play in the Tumor Microenvironment. *Cancer microenvironment : official journal of the International Cancer Microenvironment Society* 8, 3, 125–158.

[71] Takeuchi, O. and Akira, S. 2010. Pattern recognition receptors and inflammation. *Cell* 140, 6, 805–820.

[72] Taylor, R. P. and Lindorfer, M. A. 2016. Cytotoxic mechanisms of immunotherapy: Harnessing complement in the action of anti-tumor monoclonal antibodies. *Seminars in immunology* 28, 3, 309–316.

[73] Teillet, F., Dublet, B., Andrieu, J.-P., Gaboriaud, C., Arlaud, G. J., and Thielens, N. M. 2005. The two major oligomeric forms of human mannan-binding lectin: chemical characterization, carbohydrate-binding properties, and interaction with MBL-associated serine proteases. *Journal of immunology (Baltimore, Md. : 1950)* 174, 5, 2870–2877.

[74] Tenora, L., Alt, J., Dash, R. P., Gadiano, A. J., Novotná, K., Veeravalli, V., Lam, J., Kirkpatrick, Q. R., Lemberg, K. M., Majer, P., Rais, R., and Slusher, B. S. 2019. Tumor-Targeted Delivery of 6-Diazo-5-oxo-l-norleucine (DON) Using Substituted Acetylated Lysine Prodrugs. *Journal of medicinal chemistry* 62, 7, 3524–3538.

[75] Thangavelu, K., Chong, Q. Y., Low, B. C., and Sivaraman, J. 2014. Structural basis for the active site inhibition mechanism of human kidney-type glutaminase (KGA). *Scientific reports* 4, 3827.

[76] Ueki, N., Lee, S., Sampson, N. S., and Hayman, M. J. 2013. Selective cancer targeting with prodrugs activated by histone deacetylases and a tumour-associated protease. *Nature communications* 4, 2735.

[77] Uher, O., Caisova, V., Hansen, P., Kopecky, J., Chmelar, J., Zhuang, Z., Zenka, J., and Pacak, K. 2019. Coley's immunotherapy revived: Innate immunity as a link in priming cancer cells for an attack by adaptive immunity. *Seminars in oncology* 46, 4-5, 385–392.

[78] Uher, O., Caisova, V., Padoukova, L., Kvardova, K., Masakova, K., Lencova, R., Frejlachova, A., Skalickova, M., Venhauerova, A., Chlastakova, A., Hansen, P., Chmelar, J., Kopecky, J., Zhuang, Z., Pacak, K., and Zenka, J. 2021. Mannan-BAM, TLR ligands, and anti-CD40 immunotherapy in established murine pancreatic adenocarcinoma: understanding therapeutic potentials and limitations. *Cancer immunology, immunotherapy : CII* 70, 11, 3303–3312.

[79] Vonderheide, R. H. 2020. CD40 Agonist Antibodies in Cancer Immunotherapy. *Annual review of medicine* 71, 47–58.

[80] Wang, S.-Y., Veeramani, S., Racila, E., Cagley, J., Fritzinger, D. C., Vogel, C.-W., St John, W., and Weiner, G. J. 2009. Depletion of the C3 component of complement enhances the ability of rituximab-coated target cells to activate human NK cells and improves the efficacy of monoclonal antibody therapy in an in vivo model. *Blood* 114, 26, 5322–5330.

[81] Wang, Y., Bai, C., Ruan, Y., Liu, M., Chu, Q., Qiu, L., Yang, C., and Li, B. 2019. Coordinative metabolism of glutamine carbon and nitrogen in proliferating cancer cells under hypoxia. *Nature communications* 10, 1, 201.

[82] Wise, D. R. and Thompson, C. B. 2010. Glutamine addiction: a new therapeutic target in cancer. *Trends in biochemical sciences* 35, 8, 427–433.

[83] Wise, D. R., Ward, P. S., Shay, J. E. S., Cross, J. R., Gruber, J. J., Sachdeva, U. M., Platt, J. M., DeMatteo, R. G., Simon, M. C., and Thompson, C. B. 2011. Hypoxia promotes isocitrate dehydrogenase-dependent carboxylation of α-ketoglutarate to citrate to support cell growth and viability. *Proceedings of the National Academy of Sciences of the United States of America* 108, 49, 19611–19616.

[84] Xiong, S., Dong, L., and Cheng, L. 2021. Neutrophils in cancer carcinogenesis and metastasis. *Journal of hematology & oncology* 14, 1, 173.

[85] Zhang, P., Zhai, Y., Cai, Y., Zhao, Y., and Li, Y. 2019. Nanomedicine-Based Immunotherapy for the Treatment of Cancer Metastasis. *Advanced materials (Deerfield Beach, Fla.)* 31, 49, e1904156.

9 Appendix

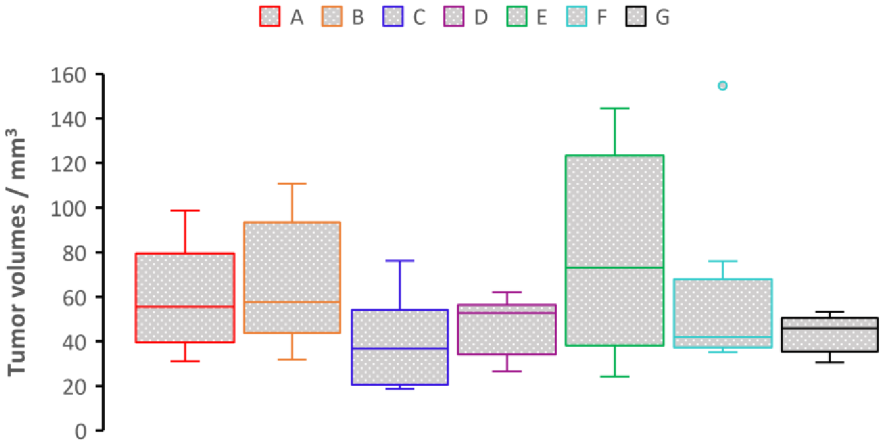

Figure 27: Box plot representing values for the right tumor distribution on day 0

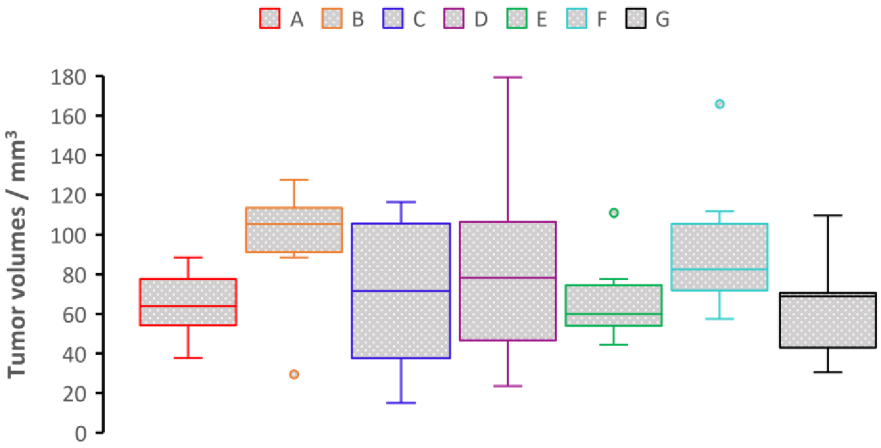

Figure 28: Box plot representing values for left tumor distribution on day 0

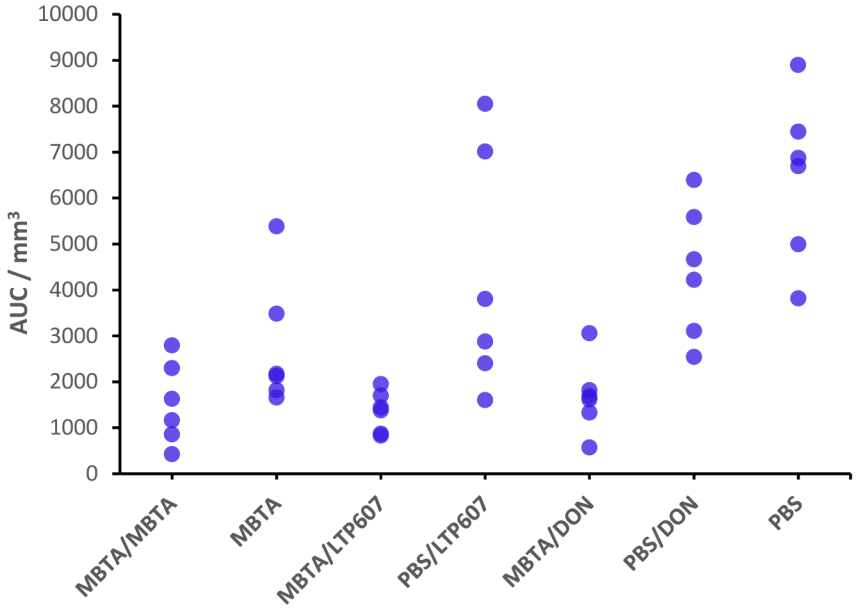

Figure 29: AUC values obtained for each group for the right tumors

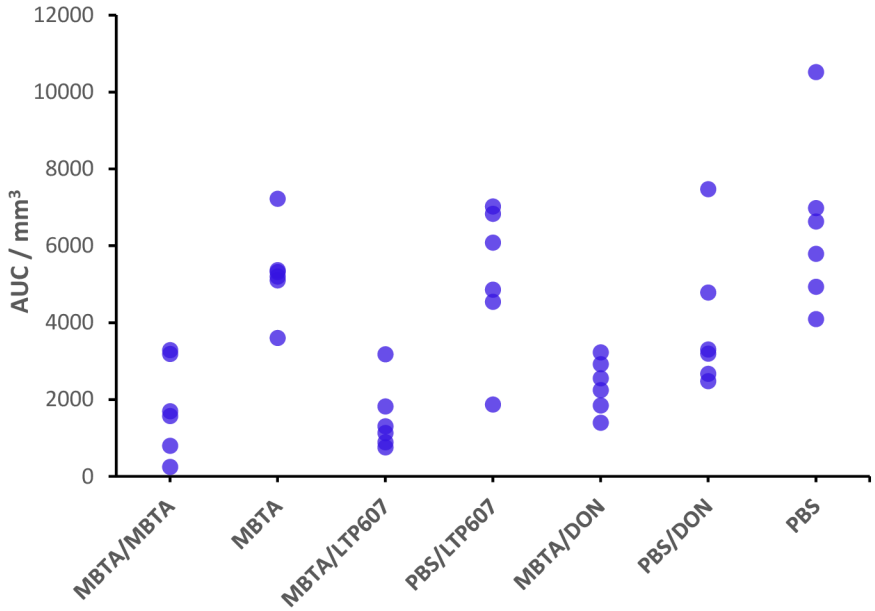

Figure 30: AUC values obtained for each group for left tumors

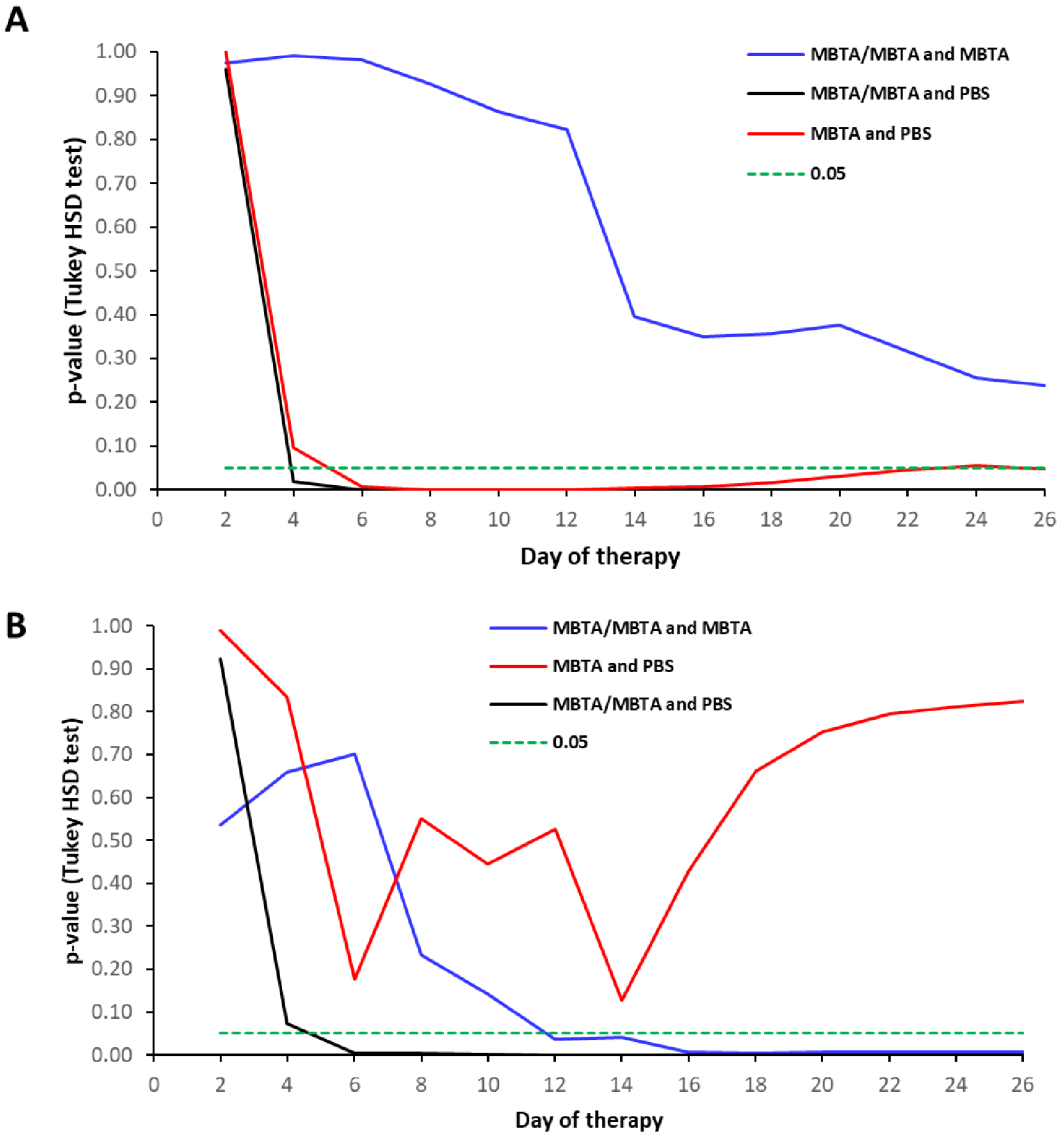

Figure 31: p-value obtained from Tukey HSD test calculated for each day of therapy: (**A**) shows the comparison for right tumors while (**B**) reflects the left tumors. Blue line describes the statistical difference between groups MBTA/MBTA (group A) and MBTA (group B), red line describes the statistical difference between MBTA (group B) and PBS (group G), finally black line represents the comparison of MBTA/MBTA (group A) with PBS (group G). Dashed green line reflects the statistically significant threshold of 0.05.

Table 4: Calculated mean tumor volume (right) in mm^3(red values show outlying values due to the death of some mice)

Day of therapy		0	2	4	6	8	10	12	14
Group	MBTA+MBTA (A)	60.44	61.73	95.65	61.54	41.65	33.43	34.07	50.32
	MBTA (B)	67.08	79.66	94.57	117.78	73.82	64.70	71.67	132.14
	MBTA+LTP607 (C)	40.59	81.20	92.95	79.52	36.53	15.58	14.45	26.09
	PBS+LTP607 (D)	46.71	90.70	128.45	238.17	111.96	91.72	115.45	141.36
	MBTA+DON (E)	80.26	82.50	83.55	120.45	59.04	29.78	26.29	53.70
	PBS+DON (F)	64.34	56.93	145.74	199.43	108.99	131.27	150.72	209.68
	PBS (G)	43.31	105.57	232.12	276.27	257.04	203.11	248.42	217.56

Table 4. Continued

Day of therapy		16	18	20	22	24	26	28	30
Group	MBTA+MBTA (A)	61.09	99.02	79.05	52.03	46.00	41.27	46.13	42.70
	MBTA (B)	94.76	163.42	138.01	184.40	90.66	100.62	113.14	131.02
	MBTA+LTP607 (C)	37.19	70.56	55.00	47.02	73.20	67.92	52.67	48.72
	PBS+LTP607 (D)	120.80	202.72	226.34	250.19	251.00	374.48	321.80	275.21
	MBTA+DON (E)	52.76	70.84	57.68	60.54	63.42	84.25	86.65	95.83
	PBS+DON (F)	191.64	237.71	202.78	234.25	188.61	246.97	192.92	234.37
	PBS (G)	270.38	270.37	258.83	351.61	290.55	540.37	408.52	392.95

Table 5: calculated mean tumor volumes (left) in mm^3(red values show outliers due to death of some mouse)

Day of therapy		0	2	4	6	8	10	12	14
Group	MBTA+MBTA (A)	64.60	79.83	105.60	72.78	85.08	43.74	33.88	35.48
	MBTA (B)	95.09	122.84	141.38	148.75	125.25	139.48	247.70	338.30
	MBTA+LTP607 (C)	69.63	75.96	95.53	89.23	67.81	25.85	41.35	44.54
	PBS+LTP607 (D)	85.21	121.14	120.27	185.27	214.40	187.30	205.91	240.86
	MBTA+DON (E)	67.77	89.52	92.72	164.20	107.16	40.68	50.78	96.68
	PBS+DON (F)	94.97	79.78	170.68	145.85	179.48	160.56	145.85	240.79
	PBS (G)	63.87	124.79	291.99	300.96	256.07	247.44	325.30	260.47

Table 5. Continued

Day of therapy		16	18	20	22	24	26	28	30
Group	MBTA+MBTA (A)	58.75	102.62	92.01	49.80	74.45	58.82	23.60	25.32
	MBTA (B)	315.01	250.90	209.32	210.36	251.63	198.22	230.07	233.64
	MBTA+LTP607 (C)	50.55	47.94	65.46	48.17	48.28	38.62	63.89	77.60
	PBS+LTP607 (D)	188.17	227.15	262.79	264.15	210.71	306.25	309.53	258.77
	MBTA+DON (E)	83.45	85.85	123.12	72.43	87.76	103.48	97.82	89.73
	PBS+DON (F)	151.39	127.95	147.26	152.70	125.18	227.30	158.69	144.88
	PBS (G)	235.80	280.90	219.28	273.72	274.11	290.01	264.05	285.76

Table 6: standard deviation (right tumor) in mm^3

Day of therapy		0	2	4	6	8	10	12	14
Group	MBTA+MBTA (A)	27.15	20.66	80.63	30.47	40.41	33.14	42.01	35.60
	MBTA (B)	32.74	27.14	43.37	81.47	49.47	59.39	68.11	121.62
	MBTA+LTP607 (C)	23.99	33.40	29.45	34.69	21.08	8.67	7.95	21.67
	PBS+LTP607 (D)	15.34	48.69	71.42	160.67	63.48	62.93	70.37	110.48
	MBTA+DON (E)	51.68	16.14	37.37	54.95	58.10	22.82	22.45	42.52
	PBS+DON (F)	46.81	22.83	39.85	60.70	40.02	92.55	70.52	143.98
	PBS (G)	9.60	36.30	92.77	85.80	87.71	53.37	93.22	63.03

Table 6. Continued

Day of therapy		16	18	20	22	24	26	28	30
Group	MBTA+MBTA (A)	41.08	61.30	50.65	65.83	60.99	35.35	53.98	60.06
	MBTA (B)	24.37	96.56	71.42	178.72	40.74	55.40	61.38	65.35
	MBTA+LTP607 (C)	22.34	63.86	44.82	36.14	55.08	49.38	49.42	45.03
	PBS+LTP607 (D)	130.41	157.43	124.26	170.18	205.38	301.14	260.68	280.30
	MBTA+DON (E)	42.08	54.06	49.13	53.10	48.95	56.73	80.16	81.20
	PBS+DON (F)	108.03	99.04	129.43	155.18	103.79	97.02	145.64	212.10
	PBS (G)	185.63	107.64	150.61	138.20	90.49	154.89	231.16	40.53

Table 7: standard deviation (left tumor) in mm^3(red values show outliers due to the death of some mice)

Day of therapy		0	2	4	6	8	10	12	14
Group	MBTA+MBTA (A)	18.79	40.79	75.61	45.43	70.31	45.23	34.45	32.14
	MBTA (B)	34.80	57.67	40.30	43.82	46.94	48.35	93.79	121.98
	MBTA+LTP607 (C)	42.63	45.55	50.49	37.91	46.19	16.82	30.02	38.12
	PBS+LTP607 (D)	56.30	37.22	41.41	79.93	100.34	127.21	94.45	115.42
	MBTA+DON (E)	23.97	39.87	62.19	83.61	63.43	47.59	43.46	51.75
	PBS+DON (F)	39.21	53.36	59.06	62.94	45.13	50.53	96.21	161.03
	PBS (G)	28.90	43.27	141.38	207.94	100.15	92.97	137.04	58.52

Table 7. Continued

Day of therapy		16	18	20	22	24	26	28	30
Group	MBTA+MBTA (A)	46.80	79.03	64.92	87.73	80.25	71.57	23.37	35.57
	MBTA (B)	191.47	117.11	115.66	84.94	118.98	121.32	161.81	200.72
	MBTA+LTP607 (C)	47.29	52.42	61.78	53.30	53.50	37.09	60.97	104.33
	PBS+LTP607 (D)	66.86	85.55	132.28	156.53	152.80	274.51	257.25	235.80
	MBTA+DON (E)	39.46	26.61	74.47	40.71	66.83	56.27	88.40	51.48
	PBS+DON (F)	111.99	84.68	125.28	127.17	117.21	188.98	105.81	121.31
	PBS (G)	109.31	140.46	159.58	137.26	117.59	101.05	68.60	90.83

Table 8: standard error of the mean (SEM) in mm^3 (right tumor) (red values show outlying due to the death of some mice values)

Day of therapy		0	2	4	6	8	10	12	14
Group	MBTA+MBTA (A)	11.08	8.44	32.92	12.44	16.50	13.53	17.15	14.53
	MBTA (B)	13.36	11.08	17.71	33.26	20.19	24.25	27.81	49.65
	MBTA+LTP607 (C)	9.79	13.63	12.02	14.16	8.61	3.54	3.25	8.85
	PBS+LTP607 (D)	6.26	19.88	29.16	65.59	25.91	25.69	28.73	45.10
	MBTA+DON (E)	21.10	6.59	15.26	22.43	23.72	9.32	9.16	17.36
	PBS+DON (F)	19.11	9.32	16.27	24.78	16.34	37.78	28.79	58.78
	PBS (G)	3.92	14.82	37.87	35.03	35.81	21.79	38.06	25.73

Table 8. Continued

Day of therapy		16	18	20	22	24	26	28	30
Group	MBTA+MBTA (A)	16.77	25.03	20.68	26.88	24.90	14.43	22.04	24.52
	MBTA (B)	9.95	39.42	29.16	72.96	16.63	22.62	25.06	26.68
	MBTA+LTP607 (C)	9.12	26.07	18.30	14.75	22.49	20.16	20.17	18.38
	PBS+LTP607 (D)	53.24	64.27	50.73	69.48	83.85	122.94	106.42	114.43
	MBTA+DON (E)	17.18	22.07	20.06	21.68	19.98	23.16	32.73	33.15
	PBS+DON (F)	44.10	40.43	52.84	63.35	42.37	39.61	59.46	86.59
	PBS (G)	75.78	43.94	61.49	56.42	36.94	63.23	94.37	16.55

Table 9: standard error of the mean (SEM) in mm^3 (left tumor) (red values show outliers due to the death of some mice)

Day of therapy		0	2	4	6	8	10	12	14
Group	MBTA+MBTA (A)	7.67	16.65	30.87	18.54	28.70	18.46	14.06	13.12
	MBTA (B)	14.21	23.54	16.45	17.89	19.16	19.74	38.29	49.80
	MBTA+LTP607 (C)	17.40	18.59	20.61	15.48	18.86	6.87	12.26	15.56
	PBS+LTP607 (D)	22.99	15.19	16.90	32.63	40.96	51.93	38.56	47.12
	MBTA+DON (E)	9.79	16.28	25.39	34.13	25.89	19.43	17.74	21.13
	PBS+DON (F)	16.01	21.78	24.11	25.69	18.42	20.63	39.28	65.74
	PBS (G)	11.80	17.66	57.72	84.89	40.89	37.96	55.95	23.89

Table 9. Continued

Days of therapy		16	18	20	22	24	26	28	30
Group	MBTA+MBTA (A)	19.11	32.26	26.50	35.81	32.76	29.22	9.54	14.52
	MBTA (B)	78.17	47.81	47.22	34.68	48.57	49.53	66.06	81.95
	MBTA+LTP607 (C)	19.31	21.40	25.22	21.76	21.84	15.14	24.89	42.59
	PBS+LTP607 (D)	27.30	34.93	54.00	63.90	62.38	112.07	105.02	96.27
	MBTA+DON (E)	16.11	10.86	30.40	16.62	27.28	22.97	36.09	21.02
	PBS+DON (F)	45.72	34.57	51.14	51.92	47.85	77.15	43.20	49.52
	PBS (G)	44.63	57.34	65.15	56.04	48.01	41.25	28.01	37.08

Table 10: statistical values (mean, SD, and SEM) for AUC

Group	Right tumor / mm^3			Left tumor / mm^3		
	Mean value	SD	SEM	Mean value	SD	SEM
MBTA+MBTA (A)	1533	895	366	1791	1232	503
MBTA (B)	2779	1430	584	5295	1152	470
MBTA+LTP607 (C)	1367	447	183	1510	896	366
PBS+LTP07 (D)	4296	2630	1074	5197	1919	783
MBTA+DON (E)	1686	808	330	2360	680	278
PBS+DON (F)	4427	1457	595	3977	1893	773
PBS (G)	6457	1802	736	6487	2244	916

Table 11: p-values for the log10 of AUC values (right tumor) analyzed with Tukey's test (statistically significant values are shown in red)

Group	A	B	C	D	E	F	G
A		0.2387	1.0000	0.0131	0.9976	0.0035	0.0002
B	0.2387		0.2557	0.8527	0.5448	0.5659	0.0468
C	1.0000	0.2557		0.0145	0.9984	0.0038	0.0002
D	0.0131	0.8527	0.0145		0.0523	0.9988	0.5149
E	0.9976	0.5448	0.9984	0.0523		0.0153	0.0004
F	0.0035	0.5659	0.0038	0.9988	0.0153		0.8143
G	0.0002	0.0468	0.0002	0.5149	0.0004	0.8143	

Table 12: p-values for AUC values (left tumor) analyzed with Tukey's test (statistically significant values are shown in red)

Group	A	B	C	D	E	F	G
A		0.0059	0.9999	0.0080	0.9948	0.2005	0.0002
B	0.0059		0.0025	1.0000	0.0314	0.7482	0.8244
C	0.9999	0.0025		0.0034	0.9589	0.1061	0.0002
D	0.0080	1.0000	0.0034		0.0411	0.8088	0.7658
E	0.9948	0.0314	0.9589	0.0411		0.5382	0.0009
F	0.2005	0.7482	0.1061	0.8088	0.5382		0.0957
G	0.0002	0.8244	0.0002	0.7658	0.0009	0.0957	

Table 13: p-values obtained for the paired T-test (red values indicate p-values less than 0.05)

Group	A	B	C	D	E	F	G
p-value	0.15825	0.00002	0.17016	0.06661	0.00077	0.12343	0.69708

Table 14: p-values obtained from the log-rank test (statistically significant values (less than 0.05) are shown in red.

Group	A	B	C	D	E	F	G
A		0.024	0.329	0.014	0.086	0.033	0.007
B	0.024		0.029	0.491	0.053	0.378	0.156
C	0.329	0.029		0.019	0.289	0.062	0.012
D	0.014	0.491	0.019		0.030	0.195	0.154
E	0.086	0.053	0.289	0.030		0.261	0.017
F	0.033	0.378	0.062	0.195	0.261		0.020
G	0.007	0.156	0.012	0.154	0.017	0.020	

Table 15: Mean AUC values relative to the value of the control group (group G)

Group	Relative mean value / %	
	Right	Left
A	23.7	27.6
B	43.0	81.6
C	21.2	23.3
D	66.5	80.1
E	26.1	36.4
F	68.6	61.3
G	100.0	100.0